Protective Role of Adiponectin in Volume Overload-Induced Heart Failure

by

Lili Wang

A dissertation submitted to the Graduate Faculty of
Auburn University
in partial fulfillment of the
requirements for the Degree of
Doctor of Philosophy

Auburn, Alabama
December 13, 2014

Keywords: adiponectin, volume overload, heart failure, myocyte contractility, intracellular Ca^{2+} handling, electrophysiological properties

Approved by

Juming Zhong, Chair, Associate Professor of Veterinary Histology
Rajesh Haresh Amin, Assistant Professor of Drug Discovery & Development
Robert L. Judd, Boshell Associate Professor of Pharmacology
Dean D. Schwartz, Associate Professor of Physiology
Ya-Xiong Tao, Professor of Physiology

Abstract

Heart failure (HF) is approaching epidemic proportions in United States. Adiponectin is a protein hormone that plays an important role in modulating glucose uptake and fatty acid β-oxidation in the heart. It has been well documented that adiponectin is able to exert protective effects on the ventricular remodeling following pressure overload and myocardial ischemia. However, the potential effect of adiponectin in volume-overload heart failure has not been reported. In addition, no study is available focusing on the potential role of adiponectin in the electrophysiological remodeling following pathological conditions.

To investigate the potential effect of adiponectin on ventricular contractile dysfunction following volume overload, we used infrarenal aorta-vena cava fistula surgery to create cardiac volume overload on rats. Our data indicated a progressive reduction of serum adiponectin level with the development of volume overload-induced heart failure. In ventricular myocytes isolated from 12-week Fistula rats, protein expression of APN, AdipoR1, AdipoR2 and T-cadherin were decreased, and AMPK activity was reduced. Consistent with these, myocytes exhibited significant depression in cell shortening and intracellular Ca^{2+} transient. *In vivo* supplementation of APN significantly increased APN serum levels, and prevented the depression of myocyte contractile performance following 12-week fistula. Moreover, *in vitro* treatment with

APN also significantly improved myocyte contractility and intracellular Ca^{2+} transient from 12-week fistula rat.

Furthermore, we analyzed the potential role of APN on the ventricular electrophysiological remodeling secondary to volume overload. Results showed that the duration of action potential was prolonged in ventricular myocytes following 10-week fistula, which was reflected by the lengthened QT interval on the surface ECG. The prolongation of action potential duration was correlated with a depression of I_{to} function as well as a decrease of I_{to} channel component expression in ventricular myocytes at 10 weeks post-fistula. In addition, the protein level of tumor necrosis factor-α (TNF-α) was significantly increased in ventricular myocytes at 10 weeks post-fistula. However, supplementation of Ad-APN increased the protein levels of I_{to} channel components and reversed I_{to} channel function in ventricular myocytes following 10-week fistula. This further restored the duration of action potential in ventricular myocytes and the QT interval on the ECG back to the normal. In addition, the administration of Ad-APN significantly reduced the protein level of TNF-α in ventricular myocytes even following 10-week fistula. These results indicated that APN can prevent the volume overload-induced ventricular electrophysiological remodeling via a decreased production of TNF-α.

Acknowledgements

First and foremost I would like to thank my advisor, Dr. Juming Zhong for his great support of my Ph.D. study and research, and for his patience, motivation, enthusiasm, and immense knowledge. His guidance helped me in all the time of research and writing of this dissertation. I could not have imaged having a better advisor and mentor for my Ph.D study. Also, he helps me through all the hard times of my study and life, especially while my family was not here.

Besides my advisor, I would like to thank my committee members, Dr. Rajesh Amin, Dr. Dean Schwartz, Dr. Robber Judd and Dr. Ya-Xiong Tao for all their help and advice on my PhD project. I appreciate Dr. Jianzhong Shen for working as my outside reader and providing valuable guidance. Last, but not the least, I would like to acknowledge Dori Miller, research assistant in our lab, for her valuable contributions and discussions to the research project. I am also thankful for the support from my parents. Without their unselfish support and encouragement, I would not be able to finish my PhD study.

Finally, my warm thanks go to Dr. Edward Morrsion for his great effort on supporting my research project, to Dr. Frank Bartol for the financial support for my conference travel from his graduate study office.

Table of Contents

List of Figures

List of Abbreviations

APN	Adiponectin
AMPK	Adenosine monophosphate-activated protein kinase
ERK1/2	Extracellular signal-regulated kinase 1 and 2
BNP	Brain natriuretic peptide
CaMKII	Calcium/calmodulin-dependent protein kinase II
IGF-1	Insulin-like growth factor (IGF-1)
AR	Aortic regurgitation
MR	Mitral regurgitation
AV fistula	Arteriovenous fistula
RAAS	Renin-angiotensin-aldosterone system
ECG	Electrocardiogram
LV	Left ventricle
ROS	Reactive oxygen species
EC coupling	Excitation-contraction coupling
SA node	Sinoatrial node
AP	Action potential

APD	Action potential duration
I_{to}	Transient outward potassium channel
Ca_v	Voltage-gated calcium channel
$I_{Ca\text{-}L}$	L-type Ca^{2+} channel
K_{IR}	Inward rectifying channel
TNF-α	Tumor necrosis factor-alpha
HMW	High-molecular-weight form of adiponectin
fAPN	Full-length adiponectin
gAPN	Globular adiponectin
TBST	Tris-Buffered Saline with 0.1% Tween-20

Chapter 1

1.1 Introduction

Heart failure, also called congestive heart failure, is becoming an epidemic health problem and leading cause of death.[1] According to a 2010 report, 825,000 new cases were diagnosed annually and approximately 5.1 million adults were suffering from heart failure in the United States.[2] Heart failure, by definition, is a progressive condition in which the heart is unable to generate sufficient cardiac output to provide the body/tissue with adequate oxygen and nutrients to meet metabolic demands. It is a clinical syndrome attributable to a multitude of biomechanical stimuli that begins with a compensatory response known as cardiac hypertrophy followed by a decompensated response that eventually results in cardiac dysfunction.[3] Heart failure is initiated after a cascade of biological events that either acutely damages the myocardium, as in the case of the myocardial infarction, or chronically deteriorates the contractility of the myocardium, as in the case of hemodynamic overload.[4, 5] Although the nature of these cardiac diseases is quite different, the common feature is the initiation of cardiac hypertrophy and maintaining of normal ejection performance. As a result, patients remain asymptomatic or minimally symptomatic throughout the compensated phase.[6-8] During the progression of compensated hypertrophy to decompensated heart failure, patients develop symptoms. Currently, therapeutic strategies cannot attenuate or reverse the remodeling process and progression to heart failure, nor can they extend the lives of patients with moderate to

severe heart failure. Therefore, understanding the pathophysiology of heart failure is a critical and crucial step for development and proper timing of novel surgical and pharmaceutical therapies, which may prevent the progression to end-stage heart failure and decrease mortality rate.

Adiponectin (APN) is a 30-kDa, 244-amino acid protein hormone that is implicated in metabolic regulation, acting via adenosine monophosphate-activated protein kinase (AMPK) phosphorylation to influence insulin sensitivity and energy metabolism. The circulating level of APN is abundant in humans as well as rodents, ranging from 3 to 30 μg/ml.[9, 10] On average, APN comprises about 0.01% of total plasma proteins in human and 0.05% in rodents.[11] It was generally accepted that APN was exclusively synthesized and secreted by adipocytes and exerts hormonal effects on myocardium in an endocrine manner. However, recent studies reveal that adult cardiomyocytes can produce APN that exerts functionally important paracrine and autocrine effects.[12-14] APN, extensively studied in metabolic diseases, exerts anti-apoptotic and anti-inflammatory activities.[15] Due to these positive actions, the role of APN in cardiovascular protection has been investigated. In the heart, APN serves as a regulator of cardiac injury through modulation of anti-inflammatory and pro-survival reactions and functions to inhibit hypertrophic remodeling.[16]

This review will focus on the pathogenesis of volume overload-induced ventricular hypertrophy and current treatment, as well as the protective effects of APN in the development of heart failure.

1.2 Concentric and Eccentric Cardiac Hypertrophy

Hemodynamic load is considered a critical determinant of myocardial performance and its phenotypic appearance.[17] In the face of hemodynamic overburden, cardiomyocytes have the ability to sense the mechanical overstretch and convert it into intracellular signals, which causes local changes in cellular morphology and global alterations in cardiac form and function.[1, 17, 18] There are two distinct types of abnormal hemodynamic load: pressure and volume overload. Although both pressure and volume overload initiate a cascade of biological events resulting in pathological cardiac dysfunction, the spatial pattern of sarcomere assembly and the intracellular growth signaling are quite different. Understanding the differences between pressure overload and volume overload hypertrophy is important in better determining appropriate therapy for the patients to improve their clinical outcome.

1.2.1 Morphometric Alterations in Response to Pressure and Volume Overload

Cardiomyocytes rapidly proliferate during fetal life but terminally withdraw from the cell cycle soon after birth.[19] It is believed that cardiomyocytes contribute to cardiac hypertrophy through an increase in cell size rather than an increase in number

when subjected to an elevated workload. Alternatively, cardiomyocytes respond to mechanical stimuli through sarcomerogenesis, the creation and deposition of new sarcomeres.[1] Under various pathological conditions, cardiomyocyte and myocardium morphology exhibit distinct variation.

Pressure overload occurs in many clinical settings, including hypertension and aortic stenosis. In response to pressure overload, the elevation of systolic wall stress (afterload) engenders sarcomere replication in parallel, which in turn increases the cross sectional area of myocyte without significant changes in cell length.[1, 20] This type of cardiomyocyte growth results in ventricular wall thickening without chamber enlargement. The fundamental response of the myocardium to an increase in afterload is termed concentric hypertrophy. Concentric remodeling allows the ventricles to normalize wall stress from the increased pressure placed on the ventricle.[18, 21] During the progression of compensated hypertrophy to decompensated heart failure, chronic pressure overload results in low cardiac output and general systolic dysfunction.[3] Diastolic dysfunction was also observed as indicated by poor compliance and reduced myocardial relaxation capabilities.[3]

Volume overload occurs in conditions such as valvular regurgitation, anemia, pregnancy and myocardial infarction. In response to cardiac volume overload, the diastolic wall stress (preload) elevates during diastolic filling and stretches

cardiomyocytes. The elevated diastolic wall stress engenders the addition of sarcomere in series, which leads to an increase in myocyte length without a significant change in cross section area.[1, 20] As a result, the increased length-to-width ratio of cardiomyocytes causes ventricular dilation with no increase or even a decrease in ventricular wall thickness. This is termed eccentric hypertrophy. This leads to an increase in ventricular mass and a concurrent elevation in stroke volume in order to compensate for pumping extra blood volume while wall stress remains normal.[18, 20] Volume overload generates high cardiac output and systolic dysfunction, while diastolic function and compliance of the ventricle is unchanged or enhanced.[3]

1.2.2 Molecular Mechanisms

In the heart, cardiomyocytes have the ability to sense physical loads. This allows the cells to transmit the physical stress into biochemical signals that alter gene expression and modify cellular structure and function.[22] Accordingly, pressure and volume overload activate the different signaling pathways to regulate myocyte growth and influence the phenotypic appearance.[18] For example, extracellular signal-regulated kinase 1 and 2 (ERK1/2) are known to be activated when subjected to almost every stress- and agonist-induced hypertrophic stimulus, thereby directing different types of cardiac growth.[23] However, a recent study from transgenic mouse models demonstrates a more complicated picture. In pressure overload, activation of ERK1/2 would work with other signaling pathways to add sarcomeres in parallel and develop concentric cardiac growth.[24]

Antithetically, in volume overload, ERK1/2 signaling pathway would protect cardiomyocytes against the mechanical stimulus that drives the cell toward elongation.[24] Accordingly, ERK1/2 activation or inactivation may be attributable to the eccentric or concentric cardiac growth.

In addition to ERK1/2-dependent signaling pathway, Toischer *et al.* specifically compared other differences in phenotypes, signaling and gene expression between volume overload- and pressure overload-induced cardiac hypertrophy *in vivo*.[25] The results suggest that the expression of brain natriuretic peptide (BNP) is elevated 7 days after subjection to pressure overload. Furthermore, the hypertrophic phenotype in pressure overload is associated with persistent activation of calcium/calmodulin-dependent protein kinase II (CaMKII), which increases L-type Ca^{2+} current and disturbs intracellular calcium transient. On the other hand, in volume overload none of these molecular pathways change, but Akt (protein kinase B) is persistently activated with the normal calcium cycling at the same time point. Consistent with these, our lab previously found that intracellular Ca^{2+} transient remains normal in cardiomyocytes in the compensated phrase of cardiac remodeling, but it is significantly depressed in the decompensated phase of heart failure.[26] Interestingly, L-type Ca^{2+} current activity does not change in volume overload. Moreover, the analysis of gene array pathway shows that volume overload selectively activates the Wnt pathway, which may influence eccentric hypertrophy via the phosphorylation of Akt.[25]

Taking together, cardiac adaptation to a pathological stimulation by volume overload differs in many ways from pressure overload. Accordingly, pressure overload increases activation of ERK1/2 and even more persistent activation of CaMKII; on the other hand, volume overload showed early activation of Wnt signaling pathway and persistent activation of Akt.

1.3 Eccentric Cardiac Hypertrophy

Volume overload, without an increased systolic stress, leads to an increased diastolic stress and initiates the eccentric hypertrophic response whereby increased ventricular size allows the ventricle to increased stroke volume.[20, 27, 28] For complete compensation in volume overload, ventricular mass should increase in proportion to volume (thickness should increase in proportion to radius) so that adequate mass is present to pump the extra volume while wall stress remains normal.

1.3.1 Differences Between Physiological and Pathological Eccentric Hypertrophy

Cardiac hypertrophy can be broadly categorized as physiological (“normal”) or pathological (“detrimental”). Physiological hypertrophy usually results from aerobic exercise, pregnancy and normal postnatal growth. This is an adaptive response to states of cardiac hyperfunction. In the face of physiological stimuli, heart growth is mediated by insulin-like growth factor (IGF-1) signaling and is paralleled by high regulation of fatty acid uptake and oxidation.[29, 30] Physiological hypertrophy is associated with normal gene

expression and proportional chamber enlargement in the absence of fetal gene program activation and fibrosis, thereby increasing the heart's pumping capacity.[31, 32] Note that physiological hypertrophy is fully reversible and non-pathological.

Pathological hypertrophy is a consequence of a persistent abnormal elevation of preload. In the face of pathological stimuli, heart growth is mediated by neurohormones (e.g. norepinephrine, angiotensin-II), which results in the activation of the fetal gene program.[29, 31, 32] Meanwhile pathological hypertrophy leads to a switch in metabolic substrate utilization from fatty acid oxidation to glucose utilization, which increases myocyte apoptosis and fibrosis. Over time, this would result in an irreversible cardiomyopathy and cardiac dysfunction. Clinically, pathological hypertrophy is associated with increased risk of heart failure and arrhythmic death.[33]

1.3.2 Pathological Eccentric Hypertrophy

Pathological eccentric hypertrophy is often a result of structural defect that creates an inefficiency of circulation, such as valve regurgitation, anemia or a shunt between the systemic vein and artery.

Aortic regurgitation (AR), also known as aortic insufficiency, occurs when there is leakage from the aortic valve backward into the left ventricle during diastole. AR usually results from a congenital lesion such as a bicuspid aortic valve, or dilation of the aortic root (often associated with hypertension or connective tissue disorders) leading to

incompetence of leaflet closure.[34] Patients with AR would be asymptomatic or minimally symptomatic during the progression of ventricular hypertrophy, but would develop symptoms only after cardiac dysfunction has been initiated.[35] When symptoms do occur, patients usually experience shortness of breath and/or chest discomfort. Chronic AR may result in irreversible damage to the myocardium, even in the absence of symptoms. AR represents a state of mixed volume and pressure overload -- the left ventricle is exposed to higher systolic and diastolic pressures. The concentric hypertrophy is due to the increased left ventricular pressure overload associated with AR, while the eccentric hypertrophy is due to volume overload caused by the regurgitation fraction.

Mitral regurgitation (MR) is the common form of valve heart disease in clinical practice. Frequent causes of mitral regurgitation are age or myxomatous degeneration, infective endocarditis, rheumatic disease or the dilation of the left ventricle (called "functional mitral regurgitation).[36] In MR, a part of the stroke volume escapes back into the atrium during ventricular systole and then re-enters the ventricle in the following cardiac cycle. Because MR occurs into the low-pressure chamber, the contracting ventricle is exposed to pure volume overload, which triggers an increase in left ventricle diameter, mass and compliance. Individuals with chrome compensated MR may be asymptomatic, with a normal exercise tolerance and no evidence of heart failure. But if severe enough (regurgitation fraction > 60%) MR would lead to heart failure or sudden death.

Systemic arteriovenous (AV) fistula is an abnormal connection between an artery and a vein. It may arise from congenital, surgically created for hemodialysis, or pathological process, such as trauma or erosion of an arterial aneurysm. Once AV fistula is formed, a large proportion of arterial blood is shunted from the high-pressure arterial side to the low-pressure venous side, thereby increasing venous return and elevating the preload in the heart. It further results in an increase of cardiac output. Over time, the demand of an increased workload leads to eccentric hypertrophy and eventually high-cardiac-output heart failure.[36, 37] Patients with chronic AV fistula often develop severe fluid retention.

Anemia is defined as deficiency of hemoglobin in the blood, which can be caused by either too few red blood cells or too little hemoglobin in the cells.[38] Chronic anemia is common among patients with heart failure, relating to increased morbidity and mortality.[39] Moreover, chronic severe anemia is known to cause high-output heart failure. In severe anemia, the viscosity of the blood falls to as low as 1.5 times that of water rather than the normal value of about 3.[38] This leads to a decrease of the systemic vascular resistance, so that more blood flows through tissues and returns to the heart, thereby significantly increasing cardiac preload. Additionally, a decrease in systemic vascular resistance causes salt and water retention and blood volume expansion.[10, 40] Moreover, anemia causes systemic vasodilation to maintain tissue oxygenation, thereby increasing venous return to the heart and further increasing cardiac output.

1.3.3 Possible Therapeutic Targets

The renin-angiotensin-aldosterone system (RAAS) is a classic endocrine system that plays a central role in the preservation of hemodynamics through the regulation of extracellular fluid volume and sodium balance. These actions are mediated through the generation of angiotensin II, the principal effector peptide in the RAAS cascade.[41, 42] Elevation in the level of circulating angiotensin II level contributes to the pathogenesis of a variety of cardiovascular diseases, including atherosclerosis, hypertension, ventricular hypertrophy, and heart failure.[42] Consequently, ACE inhibitors that interfere with the formation of angiotensin II can be effective in lowering blood pressure and reducing cardiovascular mortality and morbidity in various at-risk patient populations. Although ACE inhibitors are widely used to treat heart failure, there is emerging evidence showing that they do not effectively attenuate ventricular remodeling during pure volume overload and do not improve ventricular function.[43]

β-blockers are competitive antagonists of catecholamine binding at the β_2-adrenergic receptor, then reversing the neurohormonal effects of the sympathetic nervous system (SNS).[44] Indeed, chronic activation of the SNS decreases myocardial contractility and compensates the reduced cardiac output from the failing heart. The β-blockers are the mainstay of treatment in heart failure with reduced ejection fraction.[45] However, the administration of β-blockers increases myocardial oxygen demand and oxidative stress in myocardium; moreover, high catecholamine levels induced peripheral vasoconstriction

and increase cardiac pre- and after-load, thus exacerbating heart failure in patients with decompensated heart failure.[46]

Evidence collected from previous studies have suggested that the initial management of heart failure with β-blockers or ACE inhibitors can stabilize the patient; however, volume overload is primarily a defect of hemodynamics and the most effective therapy is surgical correction of increased hemodynamic stress.[47] However, timing of the operation is a "moving target". There is uncertainty and considerable controversy regarding the timing of surgical intervention in patients with LV volume overload. Patients often remain asymptomatic with normal LV function for many years despite the substantial LV volume overload; however, by the time symptoms develop, a large number may have developed myocardial dysfunction, placing them at a high risk for postoperative heart failure and sudden death.[48]

Surgical techniques have improved dramatically and noninvasive methods have been introduced for objective interrogation of cardiac size and function. This may allow enhancement of knowledge on new biomakers of cardiac disease onset and the symptoms of disease evolving, and develop nonsurgical procedures.[47] Traditionally, surgical correction has involved valve replacement, but there is an increasing trend towards valve repair where possible. Valve-sparing surgery while replacing or remodeling the dilated aorta is also increasingly utilized.[34]

1.3.4 Animal Models of Volume Overload

Various animal models of chronic MR have been developed to study the pathophysiology and therapeutic approaches to this condition. Dog model of MR is the most commonly used model for study. This model is induced by mitral valve chordae tendineae rupture. Chordae tendineae cutting is performed using either closed- or open-chest model. In the closed-chest model, long flexible grasping forceps are positioned percutaneously in order to tear the mitral valve chordae. In the open-chest model, cardiopulmonary bypass is performed, and either selected chordae are cut under direct visualization or a non-specified number of chordae are cut, using a metal device inserted through the left ventricular apex. Whichever model is used, MR has been found to become chronic at 3 to 6 months after the chordae rupture. The experimental models of MR are similar to the evolution occurring naturally in patients suffering from this condition. Hence, these models are useful in understanding the disease development, and in testing new therapeutic modalities. Although severe valvular regurgitation induces similar cardiac changes, heart failure syndrome is less pronounced than in AV fistula-induced overload.[36]

In addition, the model of arteriovenous (AV) fistula has been extensively used to study the functional, structural, and molecular underpinnings of volume overload-induced chronic heart failure in rodents. The creation of AV fistula leads rapidly to development of compensatory cardiac hypertrophy to maintain elevated, but largely ineffective cardiac

output. The AV fistula model recapitulates many features of human advanced heart failure, including gradual onset, elevated cardiac filling pressures, diminished “effective” cardiac output with splanchnic hypoperfusion, neurohumoral activation, and altered calcium handling with diminished cardiac energy efficiency.[49] In a rat model, AV fistula is surgically created between the infrarenal aorta and adjacent vena cava. In short, an 18-gauge needle is inserted into the exposed abdominal aorta and advanced through the medial wall into the vena cava to create a fistula. Once the needle is withdrawn, the aortic puncture site is sealed by cyanoacrylate glue. Fistula patency is visually confirmed by the pulsatile flow of oxygenated blood into the vena cava. In summary, AV fistula serves as a simple and reproducible platform to investigate the pathogenesis of heart failure and to examine efficacy of new therapeutic approaches.

1.3.5 Time Course of Cardiac Remodeling Due to Volume Overload

The pattern of volume overload-induced heart failure has been well described in the AV fistula model of rat. In this model, the progressive development of heart failure is characterized by three distinct phases of myocardial remodeling: (1) the early and adaptive phase that encompasses the first 2 weeks of AV fistula; (2) the compensatory phase continues until the rats develop the symptoms of heart failure; (3) the decompensated phase begins when hypertrophic mechanisms can no longer maintain an adequate mass to increased workload.[26]

The initial phase occurs in the first 2 weeks post-fistula, during which hypertrophic progress begins in the ventricle and the initial remodeling of cardiomyocytes is accompanied by alterations in ventricular function.[50, 51] The early response to AV fistula is characterized by increased diastolic wall stress, activation of specific signaling pathways, cardiomyocyte elongation, inflammatory infiltration and degradation of extracellular matrix which allows for the increase of the chamber size. The heart-to-body weight ratio significantly increases as early as 2 weeks post-fistula and remains elevated compared to control during the progression of eccentric cardiac hypertrophy, but AV fistula does not affect body weight.[3]

After 2 weeks of AV fistula, early phase of remodeling resolves, leaving the heart in the stage of compensated eccentric hypertrophy with still relatively preserved systolic function and enhanced diastolic function.[36] At this stage, animals show no clinical signs of heart failure, but neurohormoral activation remains elevated. Beyond 2 weeks post-fistula, the compensatory phase of ventricular remodeling begins. Although hypertrophic progress continues in the heart until rats develop heart failure, cardiac function is preserved between 2 and 5 weeks.[26, 44] The compensatory mechanisms that are activated after the initial decline in the pumping capacity of the heart are able to modulate LV function within a physiological/homeostatic range, such that the functional capacity of the patient is preserved or is depressed only minimally [8].

After a long asymptomatic stage, heart failure signs gradually develop and overt heart failure is present. At 8 weeks post-fistula, the indexed heart mass (heart/body weight ratio) increases more than twice in comparison to sham.[26] The ventricle becomes markedly dilated but relatively thin, with decreased left ventricular diameter/wall thickness ratio. The incidence of symptomatic heart failure is approximately 50%. During the progression of ventricular hypertrophy at 8 weeks post-fistula, the transition to the irreversible decompensated phase occurs. The decompensated phase is characterized by marked ventricular dilatation with increased compliance, as well as, cardiomyocyte contraction abnormalities.[26, 52] Moreover, myocardial contractility and intracellular Ca^{2+} transient were remarkably depressed in ventricular cardiomyocytes at 12 weeks post-fistula.[26]

1.3.6 Metabolic Remodeling

Normally, the heart requires a large amount of ATP to maintain its contractile function from the fatty acid oxidation in the mitochondria.[53] Alterations in cardiac energy substrate preference from fatty acid to glucose would result in a significant change in cardiac efficiency, eventually progressing to heart failure. In the early stage, cardiac remodeling is associated with normal or slightly increased fatty acid oxidation to protect the heart against stresses.[54] However, during the progression of heart failure, fatty acid oxidation and mitochondrial respiratory activities decrease, resulting in a significant drop in cardiac ATP production. In heart failure, as a compensatory response to decreased

energy metabolism, glucose uptake and glycolysis are upregulated, but this upregulation is not sufficient to compensate for a drop in ATP production. Elevated mitochondrial reactive oxygen species (ROS) generation and ROS-mediated damage, when they overwhelm the cellular antioxidant defense system, induce heart injury and contribute to the progression of heart failure.[54] In volume-overload heart failure, despite the elevation of circulating free fatty acids, myocardial triglycerides significantly reduced and the heart attenuated anti-oxidative reserve, along with the downregulated enzymes of mitochondrial fatty acid oxidation, citric acid cycle, and respiratory chain.[49]

1.3.7 Excitation-Contraction Coupling and Cardiac Ion Channels

The heart is an excitable organ that spontaneously generates the contraction and relaxation cycle driven by excitation-contraction (EC) coupling. Normally, electrical activation of the heart commences at the sinoatrial (SA) node that is able to spontaneously fire the action potential. The electrical signals arising in the SA node firstly spread across the atria and then emerge on the ventricles after a delay, in order to stimulate their contraction in time. Because cardiomyocyte are electrically coupled to their neighbors via gap junctions, the electrical signals can propagate freely and rapidly among cells in every direction. After depolarization, the electrically activated cardiomyocytes repolarize their action potential and return to their resting state.[55]

The surface ECG is a reflection of the ongoing electrical events in the myocardium.[56] On the ECG, P wave represents the atrial depolarization, which causes atrial contraction; QRS complex represents the activation of the right and left ventricular depolarization, although most of the QRS waveform is derived from the larger left ventricular musculature; positive T wave represents the repolarization of the ventricles. At the cellular level, each cardiac action potential (AP) results from the interplay of depolarizing and repolarizing ion currents. The AP shape is determined by the function of ion channels and differs between several regions of the heart. In ventricular cardiomyocytes, the AP is subdivided into 5 phases. The initial depolarization (phase 0) results from rapid activation of voltage-gated sodium (Na_v) channels. This is followed by a transient repolarization (phase 1) due to the activation of transient outward K^+ current (I_{to}) and inactivation of Na_v. Subsequently, voltage-gated calcium (Ca_v) channels open, leading to Ca^{2+} influx. During the plateau phase (phase 2), there is a balance of inward L-type Ca^{2+} current ($I_{Ca\text{-}L}$) and outward K^+ currents (primarily I_{Kr} but also I_{Ks}).[56, 57] When the Ca_v channels inactivate, the repolarizing K^+ currents predominate and the plateau phase proceeds into the final repolarization (phase 3). During this phase, the inward rectifying channels (K_{IR}) also open and contribute to return the resting membrane potential (phase 4).[56-58]

The normal pumping activity of the heart is critically dependent on the cardiac electrophysiological properties. Alteration of the electrical phenotype renders the heart

vulnerable to ventricular arrhythmias that predispose to sudden cardiac death.[57] Hence, the electrophysiological remodeling is a common feature in the experimental models of heart failure as well as in patients with heart failure, characterized by the prolongation of AP duration.[55, 57, 59] The AP prolongation results from function downregulation of outward K^+ currents,[60-62] functional upregulation of inward calcium currents and changes in Ca^{2+} current inactivation,[26, 63, 64] or increase in late Na^+ currents.[65] Our lab previously found that $I_{Ca\text{-}L}$ currents did not change in the decompensated phase of heart failure when subjected to volume overload.[26] However, knowledge of cardiac volume overload inducing electrical remodeling and prolonging APD is very limited.

1.4 Adiponectin

1.4.1 Adiponectin Structure

In humans, the APN gene is located on chromosome 3q27, a locus linked with susceptibility to type 2 diabetes and related metabolic syndrome.[66] The primary protein sequence of APN contains a signal peptide, an N-terminal collagenous domain comprising 22 Gly-X-Y repeats, and a C-terminal C1q-like globular domain.[67, 68] The three dimensional structure of the C-terminal globular domain is strikingly similar to that of tumor necrosis factor-α (TNF-α), even though there is no homology at the primary sequence level.[69]

The 30-kDa monomer of APN is able to self-assemble into three oligomers, including trimer, hexamer and high-molecular-weight (HMW) form. Trimer is the basic unit of APN oligomers.[70] It is formed through hydrophobic interactions within its globular heads of APN and further stabilized by the non-covalent interaction of the collagenous domains in a triple-helix stalk.[67] The assembly of hexameric and HMW multimers from trimer requires the formation of the disulfide bond at highly conserved cysteine residues within the N-terminus.[70, 71] The biosynthesis and secretion of APN oligomers is tightly regulated by several molecular chaperons in the endoplasmic reticulum (ER), including ERp44 (ER protein of 44 kDa), Ero1-Lα (ER oxidoreductase 1- Lα) and DsbA-L (disulfide-bond A oxidoreductase-like protein).[72, 73] In addition to these oligomeric forms, the cleavage of full-lengthen APN (fAPN) by leukocyte elastase can generate the smaller globular fragment of APN (gAPN), which increases the binding affinity of AdipoRs in cardiomyocytes.[74, 75] The various forms of APN can be detected in serum and they mediate the distinct signaling effects in the cardiovascular system.[71, 75, 76]

1.4.2 Adiponectin Receptors

APN exerts many of its cellular effects principally through binding to two receptors: AdipoR1 and AdipoR2. AdipoR1 is ubiquitously expressed and is most abundant in skeletal muscle; it has high affinity for gAPN and low affinity for fAPN.[77] AdipoR2, which demonstrates 67% sequence homology with AdipoR1, is found in many tissues at a lower level than AdipoR1. AdopoR2 has an intermediate affinity for both

gAPN and fAPN.[77] Additionally, APN oligomers can bind with AdipoR1 and AdipoR2 to trigger intracellular signaling pathways; however, there are no studies directly comparing their affinity to AdipoR1 and AdipoR2.[78] Both AdipoRs are expressed in myocardium with AdipoR1 being the predominant form.[79, 80] Expression of AdipoRs are inversely regulated by insulin through the insulin/phosphoinositide 3-kinase/Foxo1 pathways.[81]

Similar to G protein-coupled receptors (GPCR), both AdipoRs possess seven-transmembrane domains. However, they are structurally and functionally distinct from GPCRs. AdipoRs exhibit the inverted membrane topology with a cytoplasmic N terminus and a short extracellular C terminus of approximately 25 amino acids, which is opposite to the topology of all other reported GPCRs. Moreover, the two AdipoRs do not require G proteins for their activity.[11] In fact, their N-terminal cytosolic domains interact with APPL (Adaptor Protein Containing Pleckstrin Homology Domain, Phosphotyrosine-binding Domain, and Leucine-Zipper Motif).[82, 83] Under basal conditions, APPL2 occupies the N-terminus of AdipoRs and sequesters APPL1 in cytosol by forming an APPL1-APPL2 heterodimer, thus inhibiting the APN-mediated signaling pathway. Upon APN stimulation, APPL2 dissociates from AdipoRs and releases APPL1, facilitating the recruitment of APPL1 onto AdipoRs.[82] The interaction of APPL1 and AdipoRs promotes translocation of LKB1 from nucleus to cytosol and induces anchoring of LKB1 to AdipoRs-APPL1 complex.[84] Subsequently, LKB1 interaction with APPL1-AdipoRs complex leads to the promotion of phosphorylation and activation of AMPK in response

to APN.[84, 85] When AMPK is activated, translocation of GLUT4 to the cell surface is accelerated and glucose uptake into cells is increased in a PI3K (phosphoinositide 3-kinase)-independent manner.[86] In addition, activation of PFK-2 (phosphofructokinase-2) enhances glycolysis.[87] Thirdly, AMPK directly phosphorylates acetyl-CoA carboxylase 2 (ACC2) to inhibit enzymatic activity and synthesis of malonyl-CoA. In turn, lipogenesis is inhibited and β-oxidation of fatty acid is enhanced through increased CPT-1 (Carnitine Palmitoyltransferase-1) activity in the mitochondria.[86] In sum, AMPK pathway is critical for the metabolic actions of APN.

In addition to AdipoRs, the cell-surface glycoprotein T-cadherin has been identified to specifically bind the hexameric and HMW forms of APN.[88] T-cadherin is a GPI-anchored protein that lacks transmembrane and cytoplasmic domains, so it may interact with yet-unknown transmembrane adaptors to transmit the binding signals to activate the APN-mediated intracellular signaling pathways.[89]

1.4.3 Adiponectin-Mediated Cardioprotection

It has been well demonstrated that circulating APN level inversely correlates with some forms of cardiac pathogenesis, whereby low APN level in circulation increases the risk of cardiac diseases. In hypertension, a reduction in plasma APN level is accompanied by increased risk of cardiac dysfunction.[90] Consistent with this result, Fu *et al.* also observed that serum APN concentration was rapidly decreased in spontaneously

hypertensive rats during the progression of hypertension and cardiac dysfunction.[91] The reduction of serum APN levels is positively correlated with serum IL-6 level, suggesting that hypoadiponectinemia is associated with an increased inflammatory response to hypertension.[91] However, this is not always the case. O'shea *et al.* used transverse aortic constriction (TAC) techniques to create pressure overload in mice.[92] After 3 weeks of TAC, no change in serum APN was observed in comparison with control, even though TAC already induced concentric cardiac hypertrophy and led to cardiac dysfunction. However, APN deficiency exacerbates cardiac dysfunction following pressure overload. Using the APN-knockout mice, Walsh's group reported that APN deficiency results in enhanced concentric hypertrophy and increased mortality through disruption of AMPK-dependent angiogenic regulatory axis following pressure overload.[93] In response to myocardial ischemia/reperfusion, myocardial apoptosis and infarct size are markedly enhanced in APN-knockout mice due to oxidative/nitrative stress.[94] Conversely, these pathological alterations can be reversed by the *in vivo* administration of APN.[93-95] The possible mechanism is that APN protects the heart against various insults through both AMPK- and cyclooxygenase (COX)-2-dependent mechanisms.[95]

APN can also improve the contractile function of cardiomyocytes in *db/db* diabetic obese mice.[96] Cardiomyocytes from *db/db* mice displayed a depressed sarcomere shortening and an abnormal intracellular Ca^{2+} transient. Interestingly, APN treatment *in vitro* significantly improves the contractile dysfunction of cardiomyocytes in association

with restored c-Jun and IRS-1 phosphorylation signaling.[96] This in turn leads to an overall reduction in oxidative stress.[97]

Taken together the evidence from clinical and animal studies would suggest that APN possesses multiple cardioprotective effects, increasing circulating APN levels and/or enhanced APN signaling may represent a promising strategy for the treatment of various cardiac diseases. However, up to date no study has focused on the potential roles of APN in the volume overload induced heart failure.

Chapter 2

Abstract

Adiponectin has been reported to exert cardiac protective effects during ventricular remodeling following pressure overload and myocardial ischemia. However, the potential role of adiponectin in volume overload induced heart failure has not been reported. In this study, we examined the effect of adiponectin on cardiac myocyte contractile dysfunction following sustained volume overload. Volume overload induced heart failure was surgically induced in rats by infrarenal aorta-vena cava fistula. Rats were administered with or without adenoviral adiponectin (Ad-APN) at 2-, 6-, and 9-weeks following fistula creation. Serum total adiponectin levels were measured at 3 days before, 5- and 10-weeks post-fistula. Myocyte contractility and intracellular Ca^{2+} transients were evaluated at 12 weeks post-fistula. Results indicated a progressive reduction of serum adiponectin levels. In ventricular myocytes isolated from 12-week fistula rats, protein expression of adiponectin, AdipoR1/R2 and T-cadherin were decreased, and AMPK activity was reduced. Consistent with these, myocytes exhibited significant depression in cell shortening and intracellular Ca^{2+} transient. *In vivo* overexpression of adenovirus-mediated adiponectin in fistula rats significantly increased adiponectin serum levels, and prevented the depression of myocyte contractile performance. Moreover, in vitro treatment with recombinant adiponectin significantly

improved myocyte contractility and intracellular Ca^{2+} transient from 12-week fistula rats, but had no effect on myocyte performance in control and Ad-APN animals. These results demonstrate a positive correlation of adiponectin reduction and ventricular remodeling induced by volume overload. In conclusion, adiponectin plays a protective role in volume overload-induced heart failure.

Keywords adiponectin, volume overload, heart failure, myocyte contractility, intracellular Ca^{2+} handling

2.1 Introduction

The death rate attributable to congestive heart failure (CHF) has declined, but the high prevalence of disease remains an issue in the United States.[98] Mechanical stimuli in the form of pressure overload and volume overload are believed to be the major driving forces that initiate cardiac remodeling and increase the risk for development of CHF and sudden death.[1] Pressure overload is often caused by high blood pressure and aortic stenosis. Volume overload is usually induced by valvular regurgitation, chronic myocardial infarction and pregnancy. The molecular mechanisms underlying pressure overload typically induces concentric hypertrophy, while volume overload increases diastolic load and results in eccentric hypertrophy characterized by sarcomere replication in series and longitudinal cell growth. This leads to an increase in ventricular volume with little increase in wall thickness.[99] Although pressure overload- and myocardial infarction-induced cardiac hypertrophy have been well studied, there is far less known about the mechanisms causing volume overload-induced heart failure, even though is a clinically common cause of CHF. Recent animal studies demonstrated that cardiac remodeling secondary to volume overload is closely related to ATP starvation and metabolic abnormalities in myocardium, which further exacerbates the development of heart failure after volume overload.[49, 53] Previous study from our laboratory reported that rat ventricular myocytes following sustained volume overload demonstrated significant depression in cell shortening, which was associated with reduced peak intracellular Ca^{2+}

($[Ca^{2+}]_i$) transients. Abnormal myocyte contractility and $[Ca^{2+}]_i$ in these cells resulted from the deficiency of the key Ca^{2+} handling proteins including SR Ca^{2+}-ATPase and ryanodine receptors. However, the mechanism of volume overload leading to the derangement of energy metabolism in myocardium is not clear.

Adiponectin (APN) is collagen-like protein hormone circulating at a very high concentration in the range from 3 to 30 μg/ml, thus accounting for 0.01% of total plasma protein.[9, 10] Initially, APN was believed to be exclusively expressed by white adipose tissue, but recent evidence indicates that myocardium can locally produce bioactive APN.[13] In myocardium, APN functions to modulate glucose uptake and fatty acid β-oxidation via AMP-activated protein kinase (AMPK)-dependent signaling pathways.[93, 100] These physiological effects of APN are mediated via interactions with its cell-surface receptors: AdipoR1, AdipoR2 and T-cadherin. The level of circulating APN is a predictor for the development of heart failure. Low APN level in serum (hypoadiponectinemia) is associated with cardiac hypertrophy and impairments of cardiac function under pathological conditions.[101-104] APN deficiency in APN-knockout mice further exacerbates cardiac dysfunction following pressure overload induced cardiac remodeling [95, 105]. Conversely, supplementation of APN suppresses pathologic cardiac remodeling and improves cardiac function, thus protecting heart function against myocardial injury induced by pressure overload.[95, 106] However, no study has addressed the question that whether APN is beneficial or deleterious for the development of heart failure secondary

to volume overload. Therefore, the aim of this study is to examine the effects of APN on the volume overload-induced heart failure in rats.

2.2 Materials and Methods

2.2.1 Surgical preparation and APN administration

The animal use procedures were performed conforming the NIH guidelines, and the animal use protocol was approved by the Auburn University Institutional Animal Care and Use Committee. Male Sprague Dawley rats (250-300 g, ~8 weeks) were randomly divided into three groups: Control (n=6), Fistula (n=7), and Fistula+Ad-APN (n=6). Chronic volume overload was induced through infrarenal aorto-caval (AV) fistula [26]. Infrarenal aorta-vena (AV) fistula was performed on rats under O_2-isofluorane inhalation anesthesia (2%). A midline abdominal incision was performed and the abdominal aorta and inferior vena cava were exposed. An 18-gauge needle was inserted into the exposed abdominal aorta and advanced through the medial wall into the vena cava to create a fistula. The needle was withdrawn, and the aortic puncture site was sealed by cyanoacrylate glue. Fistula patency was visually confirmed by the pulsatile flow of oxygenated blood into the vena cava. Abdominal musculature and skin incisions were sutured with 3/0 catgut and autoclip. Control animals underwent similar procedure except that no aortic puncture was applied. Fistula+Ad-APN animals received Ad-APN at 2-, 6- and 9 weeks post-fistula by intravenous injection via the tail vein.

2.2.2 Analysis of total serum APN levels

Blood samples were collected from tail vein at 3 days before, 5 weeks and 10 weeks after fistula surgery. Serum was isolated by centrifugation and preserved at -80°C until analysis. Total serum APN levels were determined by rat adiponectin ELISA kit (Millipore Co. Billerica, CA).

2.2.3 Ventricle myocyte isolation

At 12 weeks post-fistula, ventricular myocytes were isolated as previously described.[26] In brief, animals were injected *i.p* of Fetal Plus 0.5 ml, and decapitated under deep anesthesia. The heart was quickly removed and perfused with oxygenated Ca^{2+}-free Krebs-Henseleit (KH) buffer (118 mM NaCl, 4.8 mM KCl, 25 mM HEPES, 1.25 mM K_2HPO_4, 1.25 mM $MgSO_4$, 11 mM Glucose, pH at 7.4) for 5 min, followed with KH buffer containing 5 mM BDM, 2 mM Carnitine, 5 mM taurine, 2 mM glutamic acid, 0.045% collagenase (Worthington; Type II, 371 U/mg), 0.01% protease (Sigma; Type XIV, 4 U/mg) and 20 μM $CaCl_2$ for approximately 15-18 min. Ventricles were then isolated from the digested heart and mechanically dispersed in 0.02 mM Ca^{2+} Kraftbrühe (KB) solution, filtered and centrifuged at 15 g for 5 min at room temperature. Isolated cardiomyocytes were then resuspended in KH buffer with gradually increasing concentrations of Ca^{2+} to yield Ca^{2+}-tolerant cells.

2.2.4 Measurement of myocyte contractility and intracellular Ca^{2+} transient

Ventricular myocytes were collected for measurement of contractility and intracellular Ca^{2+} transient using fluorescence and edge-detecting system (IonOptix, Milton, MA).[107] Cardiomyocytes were incubated with 2.5 μM fura-2/AM at room temperature for 20 min. Cells were then washed in 1.8 mM Ca^{2+} KH buffer to remove excess fura-2. Fura-2-loaded cardiomyocytes were mounted on an inverted microscope (Nikon TE, 2000, Tokyo, Japan) and perfused with 1.8 mM Ca^{2+} KH buffer by gravity (~2 ml/min) at room temperature. Only rod shaped, clearly striated, and mechanically quiescent myocytes were chosen for the study. Myocyte contraction was elicited at 0.5 Hz frequency by field stimulation. The fura-2-fluorescence was excited by collimated light beam from a 150 W Xe arc lamp. The intracellular Ca^{2+} transient was recorded by 340/380 nm ratio excitation paired with an emission wavelength at 510 nm. The Ca^{2+} transient ratio indicates the changes in free intracellular Ca^{2+} levels. The contractile function of ventricular myocytes was determined by percent change of the sarcomere shortening simultaneously with intracellular Ca^{2+} transients. Average sarcomere length within the user-determined window, was measured using the Ionoptix Ltd software that determines the average periodicity of the Z-line density based on the fast Fourier transform algorithm. Sarcomere shortening was calculated as the difference between peak systolic length and maximum diastolic length. In some studies, ventricular myocytes isolated from different groups were incubated with 2.5 μg/ml recombinant APN for 2 h in 1.8 mM Ca^{2+} KH buffer at room temperature.

2.2.5 Western blot

Cell lysates were prepared from myocytes isolated from rats in each group. The total protein contents were determined by Bradford method. Equal amounts of protein for each sample were boiled in Laemmli buffer containing 5% β-Mercaptoethanol. Proteins were resolved by 10% SDS-PAGE gel and electrophoretically transferred to nitrocellulose membranes (Bio-Rad, Hercules, CA). Membranes were blocked in Li-Cor Odyssey blocking buffer (Lincoln, NE) for 1 hour and incubated overnight with primary antibody against target proteins. Membranes were washed three times with Tris-Buffered Saline with 0.1% Tween-20 (TBST) and incubated with infrared-conjugated secondary antibodies (Lincoln, NE) for 1 hour. Following three washes with TBS-0.1% Tween-20, blots were imaged and quantified using the Odyssey Infrared Imaging System (Li-Cor, Lincoln, NE). The target proteins were normalized to β-Actin or GADPH.

2.2.6 Materials

Recombinant adiponectin was purchased from Phoenix Pharmaceuticals, Inc. (Burlingame, CA). APN antibody was from Abcam, Inc. (Cambridge, MA). AdipoR1, AdipoR2 and T-cadherin antibodies were from Santa Cruz Biotechnology, Inc. (Santa Cruz, CA). Phospho-AMPKα (Thr172) and total AMPKα antibodies were purchased from Cell Signaling (Danvers, MA). His-tag adiponectin recombinant adenovirus was from Eton Bioscience Inc. IRDye secondary antibodies were from Li-Cor (Lincoln, NE). All chemicals were analytical grade and were from Sigma-Aldrich.

2.2.7 Statistical analysis

Myocyte contractility and intracellular Ca^{2+} transient experiments were performed on five to seven myocytes randomly chosen from each animal in each group and data averaged to represent that animal. Values were expressed as mean ± SEM and n as the number of animals studied. Data from the different groups of animals were compared using two-tailed unpaired Student's-test, and one-way ANOVA with a Student-Newman-Kuels posttest, whenever appropriate. P value of < 0.05 was considered to be significantly different.

2.3 Results

2.3.1 Total APN levels were decreased with the development of ventricular remodeling following fistula

To clarify whether circulating APN levels are inversely correlated with the progression of heart failure induced by AV fistula, ELISA assay was applied to measure serum total APN levels in all groups of rats at 3 days before, 5 weeks and 10 weeks after fistula. At 3 days before fistula, no significant difference in serum APN levels was observed between rats from different groups (data not shown). At 5 weeks and 10 weeks post-fistula, serum APN levels were significantly reduced in fistula rats. *In vivo* administration of Ad-APN significantly increased the total APN levels in serum at 5 weeks and 10 weeks post-fistula, as compared with control and fistula rats (Figure 2-1a).

Similar to the reduction of serum APN levels, the protein expression of total APN was significantly reduced in ventricular myocytes isolated from fistula rats at 12 weeks post-fistula. However, Ad-APN administration markedly increased myocardial total APN levels in fistula+Ad-APN myocytes compared with myocytes from fistula rats. No significant difference was observed in the myocardial protein APN levels between fistula+Ad-APN and control rats (Figure 2-1b).

2.3.2 Protein expression of APN receptors were depressed in ventricular myocytes at 12 weeks following fistula

AdipoR1 and AdipoR2 serve as predominant APN receptors and mediate glucose uptake and fatty acid oxidation in myocytes.[77] In addition to AdipoR1 and AdipoR2, T-cadherin has also been identified as a membrane receptor for hexameric and high-molecular-weight forms of APN, which is also critical for APN-dependent energy metabolism in myocytes.[88, 89] Western blot analysis was applied to determine the protein levels of AdipoR1/R2 and T-cadherin in isolated ventricular myocytes at 12 weeks post-fistula. Results demonstrated that myocardial protein expressions of AdipoR1/R2 and T-cadherin in the fistula group of rats were decreased at 12 weeks post-fistula as compared with control. Conversely, Ad-APN treatment prevented the reduction of receptor proteins. Myocardial protein expression of AdipoR1/R2 and T-cadherin in myocytes isolated from fistula+Ad-APN rats was comparable to that in myocytes from control rats (Figure 2-2).

2.3.3 Myocardial AMPK activation was depressed in ventricular myocyte at 12 weeks post- fistula

APN functions to mediate myocardial glucose uptake and fatty acid oxidation as well as to provide cardioprotective roles by increased AMPK activity through phosphorylation of AMPK-α (Thr172).[108] In this study, western blot was used to assess the phosphorylation status of AMPK at threonine residue 172 of its α subunit in myocytes from rats in each group. At 12 weeks post-fistula, AMPK-α phosphorylation was significantly decreased, while the total AMPK level was similar in fistula myocytes when compared to control. However, Ad-APN treatment significantly improved AMPK-α phosphorylation in myocytes from fistula+Ad-APN rats compared with in fistula myocytes. There was no significant difference of AMPK-α phosphorylation in myocytes between fistula+Ad-APN and control rats (Figure 2-3).

2.3.4 Myocyte contractile performance was decreased following 12-week fistula

To investigate the effects of APN on myocyte contractile performance when subjected to volume overload, we compared the myocyte shortening among different groups of animals. The resting sarcomere lengths were comparable among different groups of myocytes. When myocytes were electrically stimulated at 0.5 Hz, mechanical properties showed that contractile performance was depressed in myocytes from Fistula rats as compared with control at 12 weeks post-fistula. Sarcomere shortening was

significantly decreased in myocytes isolated from 12-week fistula rats. Similarly, fistula myocytes had a delayed relaxation as shown by the prolonged sarcomere relengthening when compared with that of control. *In vivo* Ad-APN administration prevented normal contractile dysfunction induced by fistula, and the contractile performance of myocytes from fistula+Ad-APN rats was not significantly different from the control myocytes (Figure 2-4).

To further examine the effects of APN on the myocyte performance at cellular levels, myocytes isolated from different groups of rats were treated with or without 2.5 μg/ml recombinant APN for 2-4 hours before mechanical study. Pretreatment with recombinant APN significantly augmented the contractility of fistula myocytes and brought the cell shortening to the normal levels of control myocytes. On the other hand, recombinant APN treatment did not affect the contractile performance in myocytes from fistula+Ad-APN and control rats (Figure 2-4).

Consistent with contractile properties, intracellular Ca^{2+} transient was also depressed in fistula myocytes. Resting fura-2 ratios were similar among different groups of myocytes. However, the peak fura-2 ratio was significantly lower, and the time-to-50% fura-2 ratio decay was remarkably prolonged in fistula myocytes compared with control. Conversely, Ad-APN treatment retained intracellular Ca^{2+} transient in myocytes from fistula+Ad-APN rats (Figure 2-5). *In vitro* treatment of myocytes with recombinant APN

restored the reduction of intracellular Ca^{2+} transient in fistula myocytes to normal values of control myocytes, but did not affect the Ca^{2+} transient in myocytes from control and fistula+Ad-APN rats (Figure 2-5).

2.4 Discussion

To our knowledge, our study is the first to demonstrate the inverse relationship between APN levels and the progression of heart failure due to sustained volume overload. One of the key findings from this study is a progressive and significant reduction of APN levels in serum and ventricular myocytes following volume overload. In addition, protein expression of APN receptors were decreased in ventricular myocytes isolated from fistula rats at 12 weeks post-fistula, which was accompanied by reduced AMPK activation. Consistent with these findings, ventricular myocyte contractility and intracellular Ca^{2+} transients were markedly depressed at 12 weeks post-fistula. Conversely, *in vivo* administration of adenovirus-mediated overexpression of APN restored the APN levels, prevented the loss of protein expression of APN receptors, enhanced AMPK phosphorylation in myocytes from fistula+Ad-APN rats, and restored the contractile performance of ventricular myocytes. Moreover, *in vitro* treatment of ventricular myocytes from fistula rats with recombinant APN fully compensated the contractile deficiency, while treatment of recombinant APN does not have any effect on the contractile performance in myocytes isolated from control and fistula+Ad-APN rats.

Cardiac remodeling involves molecular, cellular and interstitial changes. Cardiac hypertrophy is a common type of cardiac remodeling following pathological stimulation and a major predictor of the development of heart failure.[109] Abnormal mechanical stimuli in the form of pressure overload and volume overload are believed to be the major driving forces that initiate cardiac remodeling and increase the risk for development of CHF and sudden death.[1] In response to pressure and volume stress, hypertrophic growth develops in two different ways: (1) concentric hypertrophy, due to pressure overload, is characterized by a relative increase in myocyte cross sectional area without a significant change in myocyte length. It leads to reduced ventricular volume and increased wall thickness; (2) eccentric hypertrophy, in response to volume overload, results in a relative increase in myocyte length without a significant change of cross section area. This causes dilatation and thinning of the heart wall.[1, 110] At the molecular level, signaling analysis demonstrated striking differences in transducing signaling pathways that were activated under the different overload conditions. Pressure overload-induced cardiac hypertrophy is associated with increased activation of extracellular-signal-regulated kinases 1/2 (ERK1/2) and persistent activation of Ca^{2+}/calmodulin-dependent protein kinase II (CaMKII).[25, 109] On the other hand, volume overload stimulates activation of the MEK5-ERK5 signaling branch of the greater mitogen-activated protein kinases (MAPKs) [109] and Akt activation without much fibrosis signaling.[25] In addition, a total of 157 mRNAs and 13 microRNAs were differentially regulated in pressure-overload versus volume-overload mice models of heart failure.[25] In the present study, experimental data indicated

a progressive and significant reduction of APN levels in serum and ventricular myocytes following volume overload. On the other hand, serum level of APN remained the same after pressure overload challenge,[92] while APN deficiency in APN knockout mice exacerbated cardiac dysfunction following pressure overload.[93, 105] Taking together, our study further support the distinct phenotype differences between different mechanical stresses, indicating the requirement for specific pharmacological interventions for specific phenotype.

APN is a protein hormone that functions to improve insulin sensitivity and modulate energy metabolism in tissues.[111] Different from most other adipocytokines, circulating APN levels are negatively correlated with body mass index.[112] Hypoadiponectinemia has been observed in obesity and its related diseases, including hypertension, type II diabetes and coronary heart disease.[101-104, 113] Interestingly, although serum APN levels remain relatively stable in mice subjected to pressure overload.[92] APN deficiency exacerbates cardiac dysfunction following pressure overload.[90, 93] Conversely, APN supplementation prevents cardiac remodeling and ameliorates cardiac abnormalities due to pressure overload and myocardial infarction.[95, 105]

Many studies have demonstrated cardioprotective effects of APN in heart failure caused by pressure overload or myocardial infarction, but its effects on the progression of volume-overload heart failure have not been examined. Rats are the most common

animal model used to create AV fistula in order to induce eccentric hypertrophy and volume-overloaded heart failure.[114] Creation of the infrarenal AV fistula results in volume overload, which causes cardiac dilation and eccentric hypertrophy. Over time, this would lead to heart failure and increased mortality. The AV fistula model of heart failure is characterized by three distinct phases of myocardial remodeling. The initial phase occurs in the first 2 weeks post-fistula, during which hypertrophic progress begins in the ventricle and the initial remodeling of cardiomyocytes is accompanied by alterations in ventricular function.[50, 51] Beyond 2 weeks post-fistula, the compensatory phase of ventricular remodeling begins. Although hypertrophic progress continues in the heart until rats develop heart failure, cardiac function is preserved between 2 and 5 weeks.[26, 51] A previous study demonstrated that myocyte function in 5-week fistula rats was comparable with control,[26] but our study showed that serum APN levels were decreased in 5-week fistula rats. With the progression of ventricular hypertrophy at 8 weeks post-fistula, transition to the irreversible decompensated phase occurs. The decompensated phase is characterized by marked ventricular dilatation with increased compliance, as well as myocyte contraction abnormalities.[26, 52] At 10 weeks post-fistula, our study found that serum APN level was lowered in fistula rats as compared with control. Moreover, myocardial contractility and intracellular Ca^{2+} transient were remarkably depressed in ventricular myocytes at 12 weeks post-fistula. Hypoadiponectinemia may be a contributing factor to the progression of heart failure induced by volume overload. In accordance with this hypothesis, our data clearly showed that adenovirus-mediated

overexpression of APN increased serum APN levels in either 5-week or 10-week fistula rats. Following 12-week AV fistula, adenovirus-mediated APN overexpression prevented the volume overload-induced damages in cardiomyocytes and preserved contractile function of myocytes in fistula rats *in vivo*. Furthermore, APN supplementation fully recovered contractile dysfunction in 12-week fistula myocytes *in vitro*, which was in consistent with a previous report focusing on the effect of APN on the cardiomyocyte contractile function in diabetic, obese mice.[96] Although previous studies revealed that high levels of APN were associated with increased mortality and severity of congestive heart failure,[115, 116] our observations suggested that APN offers cardiovascular protection in volume-overload cardiomyopathy. However, it raises an interesting question concerning the underlying mechanism.

APN is mainly expressed by adipocytes. However, cardiomyocytes are capable of synthesizing and secreting a small amount of APN.[13, 14] Circulating APN seems to act as the predominant ligand for myocardial APN receptors and exert cardioprotective actions in an endocrine manner. Shibata *et al.* described that APN accumulated in heart following ischemia-reperfusion injury through leakage from the vascular compartment and APN protein was only detectable in injured hearts but not sham-operated hearts.[117] However, recent studies found that the locally produced APN can also mediate cardioprotection in paracrine and autocrine manners.[13, 14, 79] Guo *et al.* reported that cardiac APN protein expression did not change in STZ-induced diabetic rats, whereas

plasma APN level was decreased.[118] Conversely, our study provided evidence that APN protein was detectable in control myocytes and total APN level was significantly decreased in ventricular myocytes at 12 weeks post-fistula, which was in parallel with a decrease in serum APN level. This indicates that the protein expression of tissue and systemic APN may be regulated by the same mechanisms. However, the underlying mechanism is as yet unknown. One possible reason is the increased production of tumor necrosis factor-α (TNF-α). Our preliminary data showed that TNF-α was not detectable in control myocytes. However, TNF-α levels were elevated in ventricular myocytes at 12 weeks post-fistula. Also, TNF-α levels were significantly increased in serum when animals were subjected to volume overload.[119, 120] TNF-α may suppress APN expression via JNK (c-Jun N-terminal kinase)- and protein kinase C (PKC)-dependent signaling pathways.[121, 122] Moreover, TNF-α inhibits APN expression via TNF receptor type 1.[123]

APN has been described as achieving these protective effects through receptors, AdipoR1/R2, both of which are expressed in cardiomyocytes.[80, 118, 124] In addition to AdipoR1/R2, T-cadherin has recently been identified as a receptor for hexameric and high-molecular-weight (HMW) forms of APN.[88] Although lacking transmembrane and cytoplasmic domains, T-cadherin may act as coreceptor to transmit APN-mediated metabolic signals via an unidentified signaling pathway, further protecting myocardium against injury.[89] Cardioprotective effects of APN are determined by the protein expressions of AdipoR1/R2 and T-cadherin. Caselli *et al.* reported that the mRNA

expression of AdipoR1 was significantly upregulated and myocardial AdipoR2 and T-cadherin mRNA expression did not change in a porcine dilated cardiomyopathy model.[125] Also, AdipoR2 protein levels did not change in diabetes mellitus.[118, 126] In this study, the protein expression of AdipoR1/R2 and T-cadherin were all downregulated in ventricular myocytes following 12 weeks fistula, which was accompanied by contractile dysfunction in rats with volume-overloaded heart failure. However, adenovirus-mediated APN overexpression significantly prevented the reduction of myocardial expressions of APN receptors after 12 weeks fistula, which dramatically rescued the abnormal myocardial contractile function due to volume overload. However, the precise mechanism for depressing the myocardial expression of AdipoR1/R2 and T-cadherin is as yet unknown. A previous study showed that TNF-α functions as a negative regulator of AdipoR1/R2 expression.[79] APN overexpression may inhibit the production of TNF-α, further improving the expression of AdipoR1 and AdipoR2 in 12-week fistula cardiomyocytes. Furthermore, some studies suggested that insulin reduces AdipoR1 and AdipoR2 expression via the phosphoinositide 3-kinase/Foxo1-dependent pathway *in vivo* and *in vitro*.[81, 124]

AMPK is a stress-activated protein kinase that mediates glucose uptake and fatty acid oxidation in cardiomyocytes.[100, 127] APN functions to attenuate cardiac hypertrophy mainly through AMPK-dependent signaling pathways.[105] AMPK deficiency exacerbated myocardial hypertrophy and dysfunction.[93, 128, 129] Myocardial AMPK activity was

enhanced when subjected to short-term pressure overload and myocardial ischemia.[130, 131] Although we did not test AMPK activity in the early stage of volume overload, our study showed that AMPK activity was significantly decreased in 12-week fistula myocytes. This observation suggests that decreased AMPK activity is a decompensated mechanism that fails to satisfy cardiac energy demand and maintain energy homeostasis in the heart under volume overload and contributes to myocardial hypertrophy and myocyte abnormalities. This mechanism may be partly contributed to hypoadiponectinemia and the decreased myocardial expression of APN due to volume overload. In accordance with this, adenovirus-mediated APN overexpression increased APN levels in serum and in myocytes after 12 weeks fistula, thus enhancing AMPK activity and restoring myocyte contractile function in 12-week fistula myocytes.

In summary, this study examined the role of APN in the volume overload-induced heart failure. Our results showed that hypoadiponectinemia played a causal role in the progression of heart failure under chronic volume overload. Furthermore, the decreased expression of APN and its receptors in myocytes resulted in myocyte contractile abnormalities via the reduced AMPK phosphorylation. Thus, these observations suggested a potential therapeutic application of APN in the treatment of volume overload-induced cardiac dysfunction.

Figure Legend

Figure 2-1 Total adiponectin (APN) levels with the development of ventricular remodeling following fistula **a** serum total APN levels at 5 weeks and 10 weeks post-fistula **b** and **c** myocardial protein expression of APN normalized to β-actin in the rat model of heart failure at 12 weeks post-fistula with or without the treatment of adenovirus-APN (Ad-APN). Results were presented as mean ± SEM for Control (n=6), Fistula (n=7) and Fistula+Ad-APN (n=6). * $P<0.05$ compared with Control; # $P<0.05$ compared with Fistula+Ad-APN.

Figure 2-2 Myocardial protein expression of AdipoR1, AdipoR2 and T-cadherin in the rat model of volume overload-induced heart failure at 12 weeks post-fistula **a** protein expression of AdipoR1 normalized to glyceraldehyde 3-phosphate dehydrogenase (GADPH) in isolated ventricular myocytes; **b** protein expression of AdipoR2 normalized to β-Actin in the isolated ventricular myocytes; **c** protein expression of T-cadherin normalized to β-Actin in the isolated ventricular myocytes. Results were presented as mean ± SEM for Control (n=6), Fistula (n=7) and Fistula+Ad-APN (n=6). * $P<0.05$ compared with control; # $P<0.05$ compared with Fistula+Ad-APN.

Figure 2-3 AMP-activated protein kinase (AMPK) phosphorylation in the rat model of volume overload-induced heart failure at 12 weeks post-fistula **a** representative western blot of phospho-AMPKα (Thr172) and AMPKα in isolated ventricular myocytes **b** phospho-AMPKα (Thr172) normalized to AMPKα. Results were presented as mean ± SEM for Control (n=6), Fistula (n=7) and Fistula+Ad-APN (n=6). * $P<0.05$ compared with Control; # $P<0.05$ compared with Fistula+Ad-APN.

Figure 2-4 Contractile performance of ventricular myocytes with or without 2-4 hours in vitro APN treatment (2.5μg/ml) **a** resting sarcomere length **b** percentage of sarcomere shortening **c** time to 50% sarcomere relengthening. Results were presented mean ± SEM for Control (n=6), Fistula (n=7) and Fistula+Ad-APN (n=6). * $P<0.05$ compared with control; # $P<0.05$ compared with Fistula+Ad-APN.

Figure 2-5 Intracellular Ca^{2+} transient in isolated ventricular myocyte with or without in vitro APN treatment (2.5μg/ml) **a** resting fura-2 ratio (340/380) **b** peak fura-2 ratio (340/380nm) **c** time to the 50% ratio decay (s). Results were presented mean ± SEM for Control (n=6), Fistula (n=7) and Fistula+Ad-APN (n=6). * $P<0.05$ compared with Control; # $P<0.05$ compared with Fistula+Ad-APN.

Figure 2-1 Total adiponectin (APN) levels with the development of ventricular remodeling following fistula

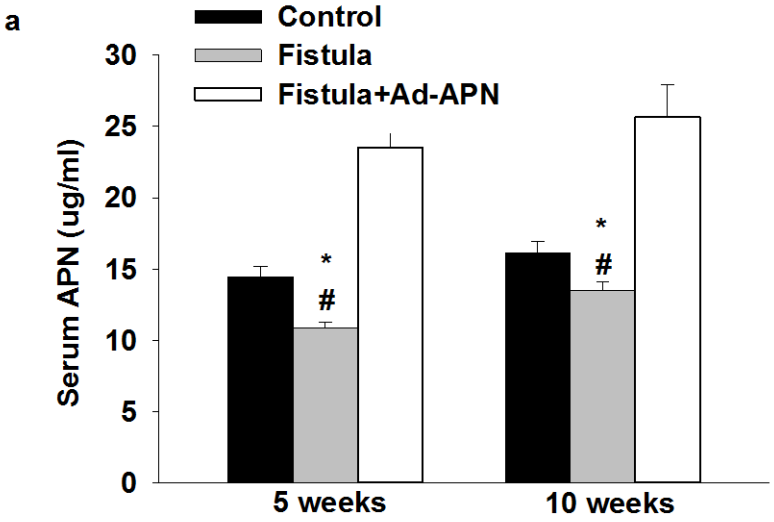
a
Control
Fistula
Fistula+Ad-APN
Serum APN (ug/ml)
30
25
20
15
10
5
0
*
#
*
#
5 weeks
10 weeks

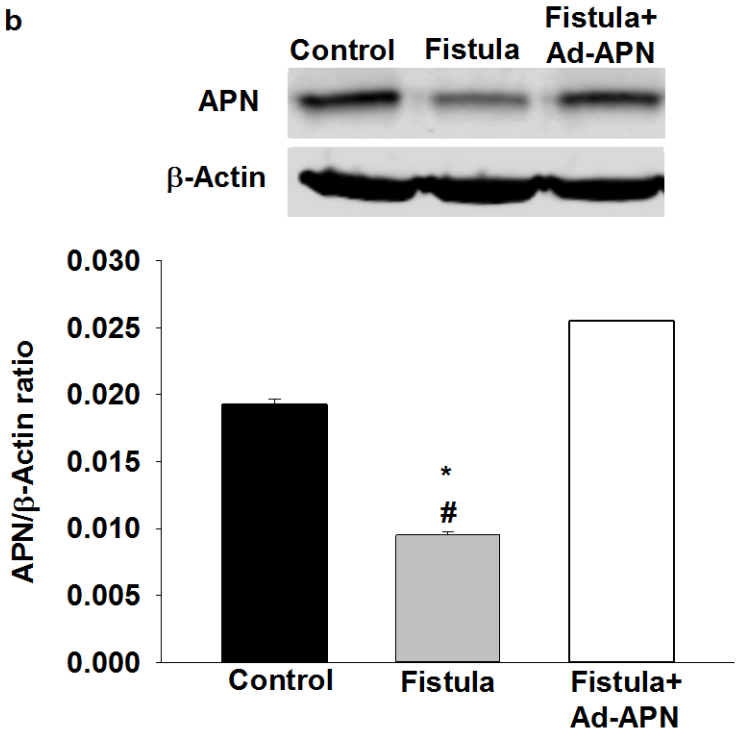
b
Control
Fistula
Fistula+
Ad-APN
APN
β-Actin
APN/β-Actin ratio
0.030
0.025
0.020
0.015
0.010
0.005
0.000
*
#
Control
Fistula
Fistula+
Ad-APN

Figure 2-2 Myocardial protein expression of AdipoR1, AdipoR2 and T-cadherin in the rat model of volume overload-induced heart failure at 12 weeks post-fistula

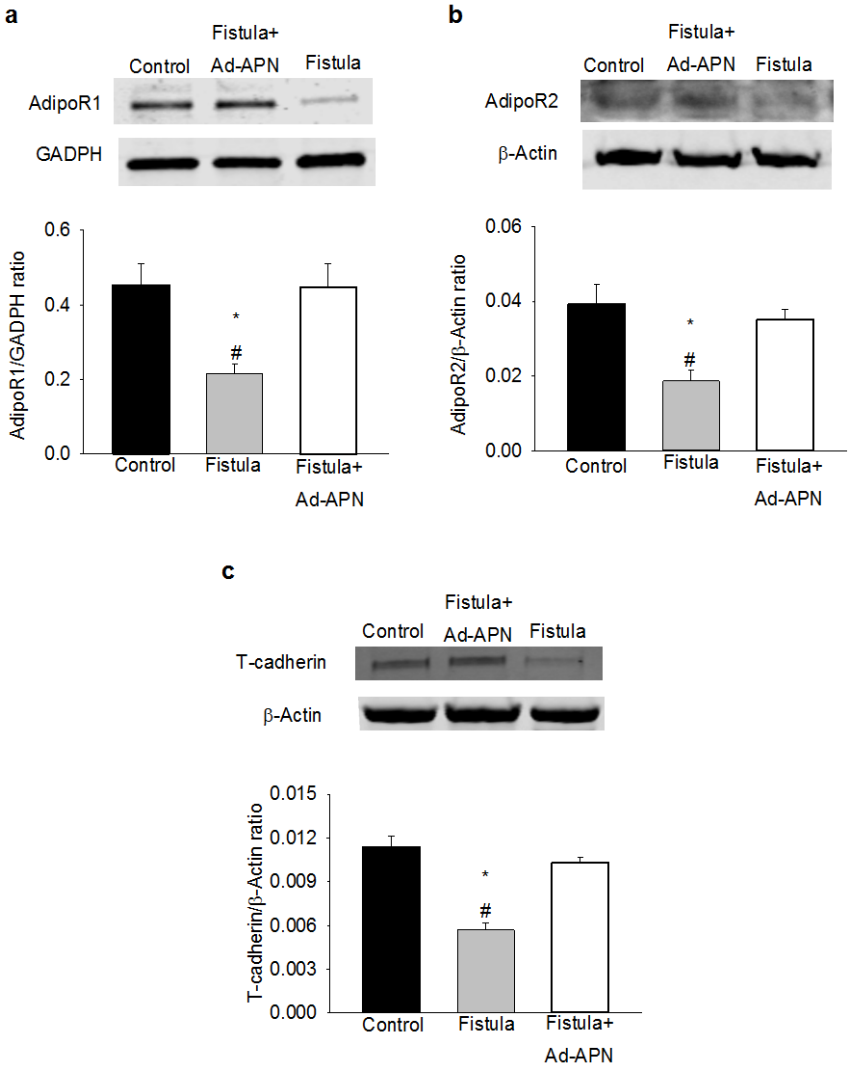
a
Fistula+
Control
Ad-APN
Fistula
AdipoR1
GADPH
AdipoR1/GADPH ratio
0.6
0.4
0.2
0.0
*
#
Control
Fistula
Fistula+
Ad-APN
b
Fistula+
Control
Ad-APN
Fistula
AdipoR2
β-Actin
AdipoR2/β-Actin ratio
0.06
0.04
0.02
0.00
*
#
Control
Fistula
Fistula+
Ad-APN
c
Fistula+
Control
Ad-APN
Fistula
T-cadherin
β-Actin
T-cadherin/β-Actin ratio
0.015
0.012
0.009
0.006
0.003
0.000
*
#
Control
Fistula
Fistula+
Ad-APN

Figure 2-3 AMP-activated protein kinase (AMPK) phosphorylation in the rat model of volume overload-induced heart failure at 12 weeks post-fistula

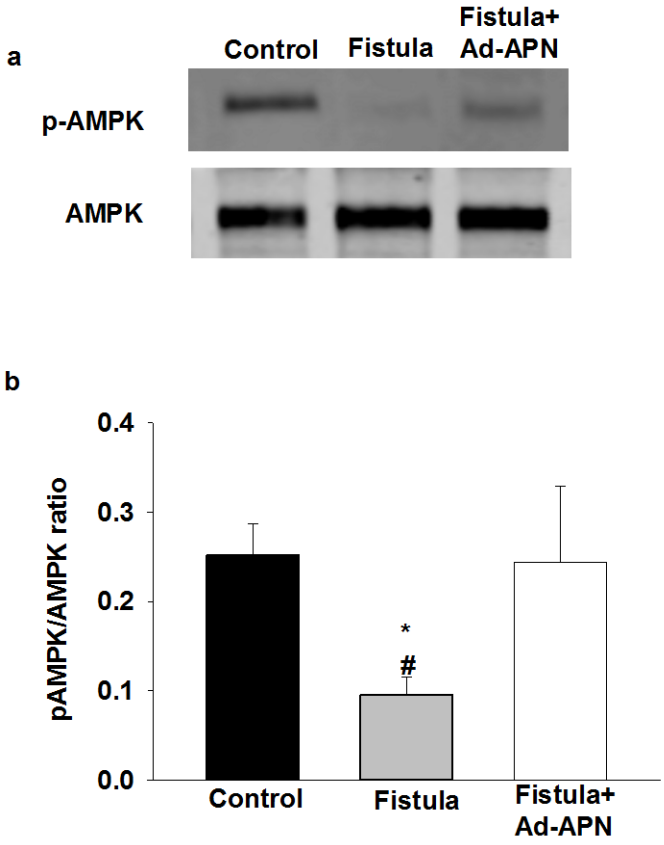
a
Control
Fistula
Fistula+
Ad-APN
p-AMPK
AMPK
b
pAMPK/AMPK ratio
0.4
0.3
0.2
0.1
0.0
*
#
Control
Fistula
Fistula+
Ad-APN

Figure 2-4 Contractile performance of ventricular myocytes with or without 2-4 hours in vitro APN treatment (2.5μg/ml)

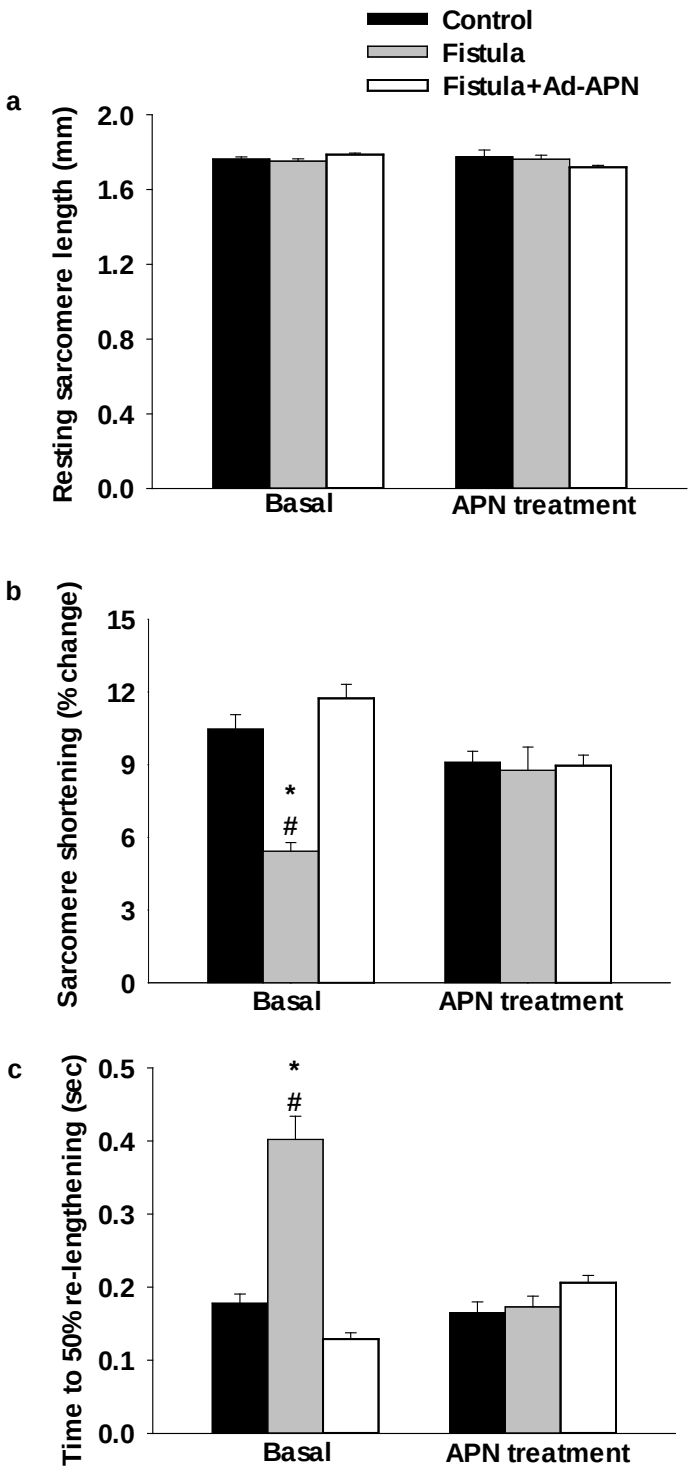
Control
Fistula
Fistula+Ad-APN
a
Resting sarcomere length (mm)
2.0
1.6
1.2
0.8
0.4
0.0
Basal
APN treatment
b
Sarcomere shortening (% change)
15
12
9
6
3
0
*
#
Basal
APN treatment
c
Time to 50% re-lengthening (sec)
0.5
0.4
0.3
0.2
0.1
0.0
*
#
Basal
APN treatment

Figure 2-5 Intracellular Ca^{2+} transient in isolated ventricular myocyte with or without in vitro APN treatment (2.5μg/ml)

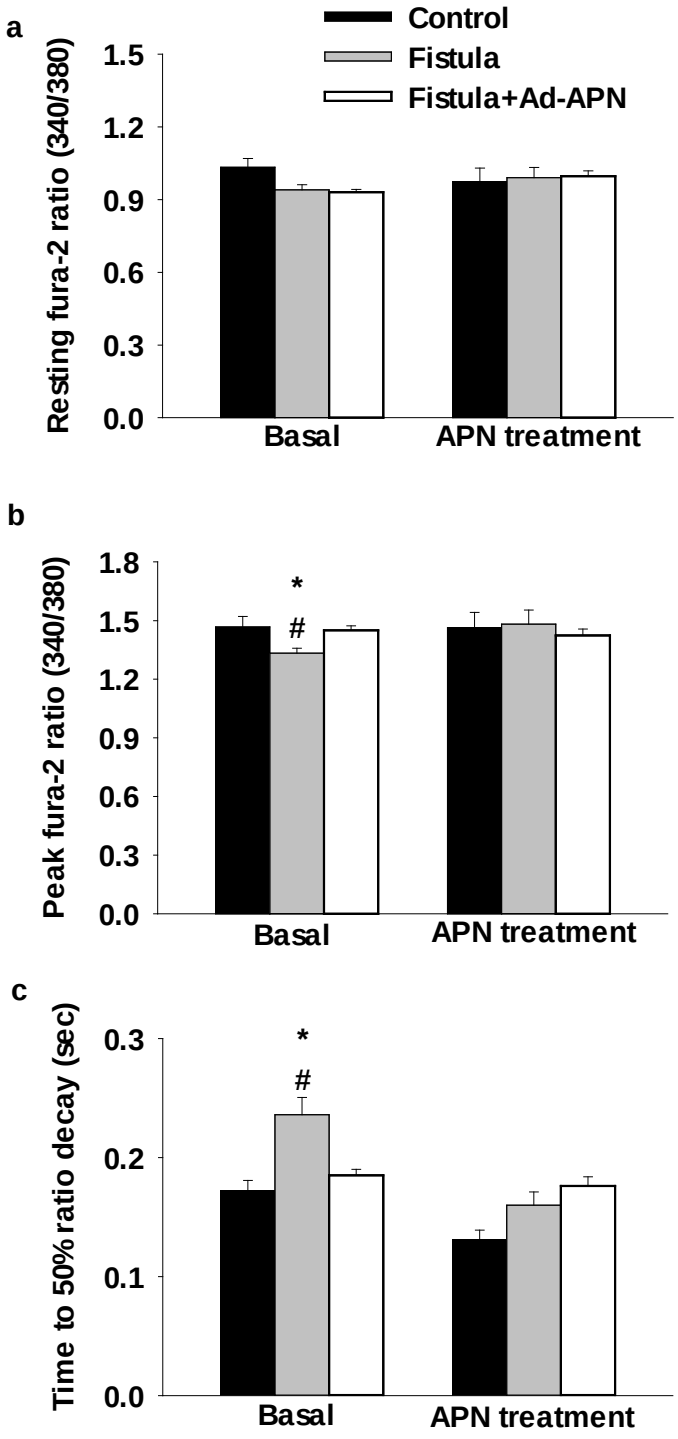
a
Control
Fistula
Fistula+Ad-APN
Resting fura-2 ratio (340/380)
1.5
1.2
0.9
0.6
0.3
0.0
Basal
APN treatment
b
Peak fura-2 ratio (340/380)
1.8
1.5
1.2
0.9
0.6
0.3
0.0
*
#
Basal
APN treatment
c
Time to 50% ratio decay (sec)
0.3
0.2
0.1
0.0
*
#
Basal
APN treatment

Chapter 3

Abstract

Adiponectin is a protein hormone that plays an important role in modulating glucose and fatty acid uptake and oxidation in the heart. Previous studies have well described the protective effects of adiponectin on ventricular remodeling in response to various pathological stimuli; however, little information is available regarding the potential effects of adiponectin on the electrophysiological remodeling under pathological conditions. In this study, we firstly analyzed the role of adiponectin on the ventricular electrophysiological remodeling secondary to volume overload by using the whole cell patch-clamp techniques and western blots. Volume-overload heart failure was induced in rats by the surgery of infrarenal aorta-vena cava fistula. After surgery, rats were administrated with adenovirus-mediated overexpression of adiponectin (Ad-APN) or GFP (Ad-GFP) at 2-, 5- and 8- weeks. Results showed that the duration of action potential was prolonged in ventricular myocytes following 10-week fistula, which was reflected by the lengthened QT interval on the surface electrocardiogram (ECG). The prolongation of action potential duration was correlated with a depression of I_{to} function as well as a decrease of I_{to} channel components expression in ventricular myocytes at 10 weeks post-fistula. In addition, the protein level of tumor necrosis factor-α (TNF-α) was significantly increased in ventricular myocytes at 10 weeks post-fistula. However, supplementation of Ad-APN increased the protein levels of I_{to} channel components and

reversed I_{to} function in ventricular cardiomyocytes following 10-week fistula. This further restored the duration of action potential and the QT interval on the ECG back to the normal. In addition, the administration of Ad-APN significantly reduced the protein level of TNF-α in ventricular myocytes even following 10-week fistula. These results indicated that adiponectin might prevent the volume overload-induced ventricular electrophysiological remodeling via a decreased production of TNF-α. This study further confirmed the cardioprotective effect of adiponectin in volume overload-induced heart failure.

Keywords adiponectin, volume-overload, cardiac electrophysiology, transient outward potassium currents

3.1 Introduction

Heart failure (HF) is approaching epidemic proportions in United States. According to a 2014 report from the American Heart Association, an estimated 5.1 million Americans suffer from HF and 825,000 new HF cases are diagnosed annually.[2] During the development of HF, the heart experiences anatomic and functional remodeling, which alters the electrophysiological properties. The electrophysiological hallmark of the failing heart is prolongation of the action potential (AP) duration (APD).[55, 57, 59] The duration and shape of AP are critically dependent on a delicate balance between the activities of depolarizing (Na^+ and Ca^{2+}) and repolarizing currents (K^+ and Cl^-). A decrease in repolarizing currents or an increase in depolarizing currents can contribute to APD prolongation, which is reflected by a lengthened QT interval on the surface electrocardiogram (ECG).[58] This further reduces the mechanical efficiency of cardiac contraction and potentially predisposes the heart to life-threatening arrhythmias. In contrast, restoration of cardiac electrical activation by cardiac resynchronization therapy can improve mechanical function and reduce mortality in HF patients.[60, 132, 133] However, the ionic mechanism that promotes ventricular remodeling is still poorly understood.

The outward potassium currents are critical to the restoration of cardiac excitability, because they play a fundamental role in modulating AP plateau and

repolarization profiles. Downregulation of the outward potassium currents is well documented to result in a prolongation of APD as well as a decrease in the early phase of AP repolarization (phase 1), presumably due to transient outward potassium currents (I_{to}).[134-137] I_{to} is a rapidly activating and inactivating 4-AP-sensitive K^+ current. In the heart, I_{to} underlies the phase 1 in cardiac AP and influences the overall AP configuration and duration. In human and animal ventricle, I_{to} is carried by channel composed of voltage-gated α subunits (a homotetramer formed by Kv4.2/4.3 channels), and auxiliary β subunit Kv channel-interacting protein 2 (KChIP2).[138] The Kv4 α subunits form the actual conductance pore and the β subunits modulate the biophysical properties of I_{to} channels. It has been suggested that HF is invariably associated with suppression of I_{to}.[134-137] The downregulation of I_{to} is closely related to a decrease in protein expression of Kv4 (including Kv4.2 and Kv4.3) as well as KChIP2.[136, 139] Despite of the importance of I_{to} in normal and diseased hearts, the underlying mechanisms for its regulation are still poorly understood.

Adiponectin (APN) is a protein hormone with respect to influence insulin sensitivity and energy metabolisms in tissues.[140] In the heart, APN is responsible for modulating glucose uptake and fatty acid oxidation via AMP-activated protein kinase (AMPK)-dependent signaling pathway.[16] Recent studies demonstrated a cardio-protective role of APN during ventricular remodeling following pathological stimulation.[16, 101-104] On the other hand, although Komatsu *et al.* found a strong inverse correlation between

serum APN and heart rate-corrected QT interval in the apparently healthy male Japanese,[141] no other study is currently available regarding the potential roles of APN on the remodeling of electrophysiological properties in ventricular myocytes. The aim of this study is to investigate the effect of APN on the ventricular electrophysiological remodeling due to cardiac volume overload.

3.2 Materials and Methods

3.2.1 Surgical preparation and treatment protocols

Male Sprague Dawley rats (250-300 g, ~8 weeks) were randomly divided into five groups: Control (n=6), Control+Ad-APN (adenovirus vector with APN, n=7), Fistula+Ad-GFP (adenovirus vector with GFP, n=4), Fistula+Ad-APN (n=8) and Fistula (n=6). Chronic volume overload was induced through infrarenal aorto-caval (AV) fistula. AV fistula was performed on rats under O_2-isofluorane inhalation anesthesia (2%). A midline abdominal incision was performed and the abdominal aorta and inferior vena cava were exposed. An 18-gauge needle was inserted into the exposed abdominal aorta and advanced through the medial wall into the vena cava to create a fistula. The needle was withdrawn, and the aortic puncture site was sealed by cyanoacrylate glue. Fistula patency was visually confirmed by the pulsatile flow of oxygenated blood into the vena cava. Abdominal musculature and skin incisions were sutured with 3/0 catgut and autoclip. Control animals underwent similar procedure except that no aortic puncture was applied. Animals in the Ad-APN and Ad-GFP groups received the adenovirus at 2-, 5-

and 8 weeks post-fistula by intravenous injection via the tail vein. The animal use procedures were performed following the NIH guidelines, and the animal use protocol was approved by the Auburn University Institutional Animal Care and Use Committee.

3.2.2 Surface electrocardiogram (ECG) recording

At 10 weeks post-fistula, surface ECG recordings were obtained from anesthetized animals. Surface ECG were recorded with silver electrodes placed on the skin at optimized positions to obtain maximal amplitude recordings. Data were recorded and analyzed using LabChart8 software (ADInstruments, Colorado Springs, CO) and QT intervals were determined; average values for individual animals were reported.

3.2.3 Ventricle myocyte isolation

At 10 weeks post-fistula, ventricular myocytes were isolated as previously described.[26] In brief, the heart was perfused with oxygenated 1.8 mM Ca^{2+} Krebs-Henseleit (KH) buffer for 3 min and Ca^{2+}-free KH buffer for 4 min, followed by perfusion with KH buffer containing 5 mM 2,3-Butanedione Monoxime, 2 mM Carnitine, 5 mM Taurine, 2 mM Glutamic acid, 0.1% Bovine Serum Albumin and 0.045% collagenase (Worthington; Type II, 285 U/mg) and 20 μM $CaCl_2$ for approximately 18 minutes and 30 seconds. Ventricles were then isolated from the digested heart and mechanically dispersed in 0.01 mM Ca^{2+} Kraftbrühe (KB) solution, filtered and settled down at room temperature. Lastly, the isolated cardiomyocytes were resuspended in 0.01

mM Ca^{2+} KH buffer with gradually increasing concentrations of Ca^{2+} to yield Ca^{2+}-tolerant cells. For all experiments, only rod-shaped myocytes with clear striations and no membrane blebs were used. Myocytes were stored in 0.5 mM Ca^{2+} KH buffer for 1 h at room temperature before the experiments and used within 8 h.

3.2.4 Electrophysiology Experiments

The whole-cell patch clamp technique was used to record action potentials and potassium currents in ventricular myocytes.[107, 142] Patch pipettes were pulled from 1.5 mm O.D. borosilicate glass capillary tubes with a PE-830 gravity puller (Narashigee, Japan) and then fire-polished with a MF-830 microforge (Narashigee, Japan). The pipette contained a silver electrode, and had a tip resistance of 2-4 MΩ when filled with appropriate pipette solution. By applying gentle suction to the pipette, a giga-seal was formed between the pipette and the cell membrane. More suction was applied to rupture the patch of membrane under the tip of the pipette, providing access for the electrode to the interior of the cell; this situation is termed the whole cell configuration. After the whole-cell configuration, cell membrane capacitance and series resistance were measured by a 20-mV hyperpolarizing pulse and partially compensated. Membrane potential and currents of myocytes were measured via the Axopatch 200B patch-clamp amplifier (Axon Instruments, CA). Currents and voltage signals were filtered at 5 kHz, collected using the data acquisition package pClamp 9 and pClamp 10 (Axon Instruments, CA). All experiments were performed at room temperature.

Action potential was recorded in current-clamp mode when myocytes were superfused with normal Tyrode solution (flow rate ~2 ml/min). Action potential was elicited by 6-ms current pulse at 20-s interval. Resting membrane potential, amplitude of action potential, and times to 50% repolarization (APD_{50}) were recorded and analyzed.

Transient outward K^+ currents (I_{to}) were measured in voltage-clamp mode. I_{to} was recorded in the presence of external 50 mM tetraethylammonium chloride (TEA-Cl), which was used to block I_K. The resting membrane potential was held at -40 mV to eliminate sodium currents. I_{to} currents were elicited by test pulses from -30 to +50 mV applied in 10 mV increments at a frequency of 0.1 Hz.

3.2.5 Western blot

Cytoplasmic and membrane protein were prepared from myocytes isolated from rats in each group, as described previously.[143, 144] The tube containing frozen myocytes were put on ice. Buffer A (50 mM Tris-HCl, 250 mM Surcose, 10 mM EGTA, 4 mM EDTA, 1 mM PMSF and 20 μg/ml Leupeptin, pH 7.5) and buffer B (buffer A with 1% Triton X-100) were prepared and chilled on ice. The myocytes were suspended in buffer A and homogenized, then transferring to 2 ml of ultracentrifuge tube and centrifuged at 33,000 rpm for 1 hour at 4°C. The supernatant was removed and represented cytosolic proteins. Pellets were resuspended in pre-chilled buffer B and incubated on ice for 1 hour to allow complete lysis of membrane proteins. Samples were centrifuged at 10,000 rpm

for 1 hour at 4°C and the supernatants were used as the membrane fraction. The protein contents were determined by using Bradford method. Protein contents were aliquoted and stored at -80°C for later analysis.

Protein lysates for each sample were reduced using Laemmli buffer containing 5% β-Mercaptoethanol. The reduced proteins were resolved in 10% SDS-PAGE gel and electrophoretically transferred to nitrocellulose membrane. The membranes were stained by Ponceau S to determine the total amount of proteins loaded on the gels. The membrane was then blocked in Tris-Buffered Saline with 0.1% Tween-20 (TBST) containing 5% nonfat dry milk for 1 hour at room temperature, and incubated with primary antibody against target proteins overnight at 4°C. Nitrocellulose membranes were washed in TBST and then incubated with IRDye Infrared Dyes (Li-Cor, Lincoln, NE) against primary antibodies. After washing with TBST, Odyssey Infrared Imaging System (Li-Cor, Lincoln, NE) was used to image and quantify the protein bands. The target proteins were normalized to Ponceau images of total proteins.

3.2.6 Materials and Solutions

GFP expressing RGD fiber modified adenovirus was from Vector Biolabs (Philadelphia, PA). His-tag APN recombinant adenovirus was purchased from Eton Bioscience, Inc. (San Diego, CA). Kv4.3 (sc-11686), Kv4.2 (sc-11680), KChIP2 (sc-25685), TNF-α (sc-1350) and GAPDH (sc-20357) antibodies were purchased from Santa

Cruz Biotechnology, Inc. (Santa Cruz, CA). IRDye secondary antibodies were purchased from Li-Cor (Lincoln, NE). All chemicals were analytical grade and were from Sigma-Aldrich.

KH buffer was composed of (in mmol/L) 118 NaCl, 4.8 KCl, 25 HEPES, 1.25 K_2HPO_4, 1.25 $MgSO_4$ and 11 Glucose, pH adjusted to 7.4 with NaOH.

KB solution included (in mmol/L) 20 KCl, 10 KH_2PO_4, 70 L-Glutamine, 10 DL-β-hydroxybutyric acid, 10 Taurine, 2.5 EGTA, 10 Glucose, 5 HEPES and 1% Bovine Serum Albumin, pH adjusted to 7.4 with KOH.

For outward K^+ current measurement, the intracellular recording pipette solution contained (in mmol/L) 80 L-aspartic acid, 50 KCl, 10 KH_2PO_4, 10 EGTA, 5 HEPES, 3 ATP-Na, 1 $MgSO_4$, pH adjusted to 7.2 with KOH. I_{to} bath solution was composed of (in mmol/L) 137 NaCl, 4.0 KCl, 1.0 $MgCl_2$, 0.5 $CaCl_2$, 10 HEPES, 2.0 $CoCl_2 \cdot 6H_2O$, and 10 Glucose, pH adjusted to 7.4 with NaOH. When 50 mM TEA-Cl was added to the I_{to} bath solution, NaCl was equimolarly substituted by TEA-Cl.

For action potential recording, the pipette solution was composed of (in mmol/L) 100 KCl, 10 NaCl, 5 ATP-Mg, 10 EGTA, 2 MgCl2, 10 HEPES, 5.5 Glucose and 0.5 GTP,

pH adjusted to 7.2 with KOH. The bath solution was (in mmol/L) 137 NaCl, 5.4 KCl, 1.0 MgCl2, 1.8 mM CaCl2, 10 HEPES and 10 Glucose, pH adjusted to 7.4 with NaOH.

3.2.7 Data analysis and statistics

All electrophysiological experiments were performed on five to six myocytes from the same animals for each protocol and data were averaged to represent that animal. Western blot were repeated in triplicate for all animals. Statistical data were presented as mean ± SEM and n as the number of animals studied. Statistical significance was evaluated by the independent Student's t-test or one-way ANOVA. Differences were regarded as significance when the p-value was <0.05.

3.3 Results

In this study, the supplementation of Ad-GFP did not affect the electrophysiological properties in ventricular myocytes at 10 weeks post-fistula. There was no significant difference observed in the APD, the QT interval and I_{to} current between Fistula+Ad-GFP and Fistula rats (data not shown). Hence, we combined the data in Fistula+Ad-GFP and Fistula groups together.

3.3.1 The duration of action potential and QT interval were prolonged following 10-week fistula

To determine the possible contribution of APN on the volume overload-induced electrophysiological remodeling at cellular level, current-clamp mode was used to record AP in ventricular myocytes from different groups. Results showed that the AP waveforms were prolonged in Fistula myocytes compared to Control myocytes (Figure 3-1a). The quantitative analysis of APD at 50% (APD_{50}) repolarization revealed significant prolongation in Fistula myocytes (13.999±2.41) compared to that in Control myocytes (6.743±1.69). The supplementation of APN reduced the APD_{50} in Fistula+Ad-APN myocytes and there was no significant difference between Fistula+Ad-APN and Control myocytes (7.395±0.68, 6.743±1.69, respectively). Interestingly, the APN supplementation did not affect the APD_{50} in Control+Ad-APN myocytes (5.701±0.938) (Figure 3-1b).

Next, to examine the effect of APN at the level of the whole organism, the surface ECG activity was measured in anesthetized animals. Analysis of the ECG parameters further confirmed a significant prolongation of QT interval in Fistula animals (0.0923±0.005) compared to Control animals (0.0813±0.0003), consistent with the prolongation of APD in Fistula myocytes. The supplementation of APN significantly shortened the QT interval in Fistula+Ad-APN animals (0.0778±0.005) and there was no significant difference between Fistula+Ad-APN and Control animals. By contrast, the

administration of APN did not affect the QT interval in Control+Ad-APN animals (0.0788±0.002) (Figure 3-2).

3.3.2 I_{to} peak current was depressed in myocytes following 10 weeks fistula

To determine the possible effect of APN on the current-voltage relationship of peak I_{to} currents in ventricular myocytes at 10 weeks post-fistula, the amplitude of I_{to} was recorded in serial test pulses from -30 to +50 mV in 10-mV increments. Following 10-week fistula, the peak I_{to} density (at +50 mV) was reduced from 13.408±1.407 to 7.47±0.497 ($P<0.05$). Furthermore, the peak I_{to} density was significantly decreased at the potentials ranging from -10 to +50 mV compared to Control ($P<0.05$). The supplementation of APN restored the peak I_{to} density in Fistula+Ad-APN myocytes, but it did not affect the peak I_{to} density in Control+Ad-APN myocytes (Figure 3-3).

3.3.3 Protein expression of I_{to} channel components were reduced in myocytes at 10 weeks following fistula

I_{to} channels are heteromultimers, composed of Kv4.2 and Kv4.3 α subunits.[61] The major function of Kv4.2 and Kv4.3 is to form the actual conductance pore and conduct the outward potassium currents. Only reduction in Kv4.2 and Kv4.3 abundance have been linked consistently to the diminished Ito densities typically seen in cardiac hypertrophy. To explore the molecular basis of I_{to} downregulation at 10 weeks pots-fistula, western blot was applied to measure the myocardial Kv4 protein levels on the

membrane and in the cytosol at 10 weeks post-fistula. Results from the western blot analysis showed that both Kv4.2 and Kv4.3 protein levels on the membrane fraction were significantly reduced in Fistula myocytes compared with control, consistent with the fistula-mediated depression of peak I_{to} current density. Similarly, the cytosolic protein levels of Kv4.2 and Kv4.3 were remarkably decreased in Fistula myocytes compared with Control.[145] Supplementation of APN rescued the reduction of Kv4.2 and Kv4.3 in Fistula+Ad-APN myocytes following 10-week fistula. Myocardial protein levels of Kv4.2 and Kv4.3 were comparable among Fistula+Ad-APN, Control and Control+Ad-APN groups (Figure 3-4).

The cytosolic KChIP2 is identified as the β subunit of I_{to} channel. Co-assembly of KChIP2 with Kv4 α subunits can regulate the cell surface expression and co-localization of I_{to} channels. In addition, KChIP2 can associate with Kv4 α subunits to modulate channel gating by slowing the rate of I_{to} inactivation at depolarizing potentials and accelerating recovery from inactivation.[146-148] This suggests that fistula-associated I_{to} remodeling is possibly related to changes in the protein levels of KChIP2. To test the hypothesis, myocardial KChIP2 protein levels were measured on the membrane and in the cytosol by using western blot. Consistent with the western-blot results of myocardial Kv4.2 and Kv4.3 protein level, a significant decrease in KChIP2 protein was observed in Fistula myocytes compared with Control. However, supplementation of APN significantly improved the KChIP2 protein level in Fistula+Ad-APN myocytes. There

was no significant difference of myocardial KChIP2 protein levels observed in the Fistula+Ad-APN, Control and Control+Ad-APN three groups (Figure 3-4).

3.3.4 Myocardial TNF-α protein level was increased at 10 weeks post-fistula

Tumor necrosis factor α (TNF-α) is a proinflammatory cytokine that is rarely detectable in the healthy heart, but is quickly increased when subjected to the external stresses.[149-151] Previous studies have well demonstrated that TNF-α can induce a depression of I_{to} function as well as a decrease of I_{to} channel components in adult cardiomyocytes.[152-154] To better understand the mechanisms of I_{to} downregulation at 10 weeks post-fistula, western blot was performed to measure the TNF-α protein levels in ventricular myocytes following 10-week fistula. The result showed that 10-week fistula led to the elevation of TNF-α protein levels in Fistula myocytes compared with Control. Supplementation of APN significantly reduced the protein levels of TNF-α in Fistula+Ad-APN myocytes. No significant difference of myocardial TNF-α protein levels was seen in the Fistula+Ad-APN, Control and Control+Ad-APN three groups (Figure 3-5).

3.4 Discussion

The present study was designed to characterize the possible effects of APN on the electrophysiological remodeling in ventricular myocytes when subjected to volume overload. This study was performed in ventricular myocytes derived from the hearts 10

weeks following fistula. Our results showed that the duration of AP was prolonged in ventricular myocytes at 10 weeks post-fistula, which in turn, produced the lengthened QT interval on the surface ECG. The prolongation of APD was associated with the suppression of I_{to} function as well as the decreased protein levels of I_{to} channel components in ventricular myocytes following 10-week fistula. However, *in vivo*, adenovirus-mediated overexpression of APN increased the protein levels of I_{to} components and reversed the I_{to} function in ventricular myocytes following 10-week fistula. Subsequently, this brought the duration of AP and the QT interval back to normal at 10 weeks post-fistula. Interestingly, supplementation of APN did not affect the electrophysiological properties in ventricular myocytes isolated from control animals.

Normal electrical conduction in the heart allows for the coordinated propagation of electrical impulses that initiate cardiac contraction. Clinically, the surface ECG detects the electrical behaviors happened at the surface of the body and translates them into a graph with voltage potential changes as P, QRS and T waves.[56] The QT interval contains both the QRS complex and T wave, comprising the time from the onset of ventricular depolarization to complete repolarization. A lengthened QT interval has been proposed as a risk factor for lethal ventricular arrhythmias, which may lead to sudden death in heart failure.[155-158] At a cellular level, the cardiac AP determines cardiac electrical activity and control of cardiac excitation-contraction coupling. From this study, it appears that Fistula animals had the lengthened QT intervals as compared with those in Control animals 10

weeks following fistula, which consistent with the prolongation of APD in Fistula myocytes. Supplementation of APN substantially shortened the QT interval and the duration of AP in ventricular myocytes when subjected to volume overload. But it did not influence the QT interval and heart rate in Control animals.

In ventricular myocytes, the AP is divided into the 4 phases. The inward Na^+ current (I_{Na}) causes the rapid depolarization (phase 0) followed by a brief period of repolarization (phase 1) due to activation of the transient outward K^+ current (I_{to}). Subsequently, the inward L-type calcium current ($I_{Ca,L}$), counterbalanced by the delayed rectifiers I_K, is responsible for the plateau (phase 2). The rapid final repolarization (phase 3) occurs in response to the closing of Ca^{2+} channels and the increase in outward K^+ currents. Finally, the inward rectifier I_{K1} is responsible for the maintenance of the resting membrane potential (phase 4). In rat, the presence of relatively large I_{to} current densities overpowers the depolarizing effects of $I_{Ca,L}$, thereby strongly modulating the excitation-contraction coupling processes and myocardial contractility as well as phase 1 repolarization.[134, 159, 160] Previous studies in animal models have consistently revealed that the downregulation of I_{to} results in the progressive slowing of phase 1 repolarization and it is the primary determinant of the AP prolongation in myocardium.[135, 160, 161] However, no study has examined the relationship between alterations of I_{to} density and the duration of AP in rat ventricular myocytes following volume overload.

This study showed that underlying the prolongation of APD in volume-overload heart failure, the peak I_{to} current density and amplitude were significantly reduced in ventricular myocytes. Consistent with the suppression of the I_{to} function in ventricular myocytes, corresponding down-regulation was observed for the protein levels of Kv4.3, Kv4.2 and KChIP2 when subjected to volume overload. Kv4.3 and Kv4.2 are the α pore-forming voltage-gated subunits largely responsible for the I_{to} current in the rat; KChIP2 is the β subunit of I_{to} channel, which is responsible for controlling the cell surface expression of I_{to} channels and regulating Kv4-mediated current amplitude.[146, 162] However, the supplementation of APN restored the I_{to} function and shortened APD, with increasing the protein levels of I_{to} channel components. Here, it raises an interesting question concerning the underlying mechanism of APN protecting the heart against the electrophysiological remodeling in response to volume overload.

APN is a protein hormone with a prominent function in improving energy metabolisms. APN suppresses the production of TNF-α via a COX 2-dependent mechanism.[163, 164] TNF-α is an inflammatory cytokine that appears to play a significant role in the pathophysiology of heart failure. In this study, our data showed that the protein levels of TNF-α were rarely detectable in ventricular myocytes isolated from Control animals. However, myocardial TNF-α protein levels were significantly elevated in animals following 10-week fistula. Advanced heart failure due to volume overload is correlated with the increased protein levels of TNF-α in ventricular cardiomyocytes.[154] It

has been well documented that TNF-α can trigger the hypertrophic-related responses through iNOS overexpression and oxidant species generation.[165] TNF-α can produce a significant reduction of I_{to} density and modifying its inactivation by reducing the protein expression of I_{to} components in rat ventricular cardiomyocytes.[152, 154, 165] Additionally, TNF-α is able to prolong the APD in rat ventricular myocytes via the downregulation of I_{to} function. However, administration of APN suppressed the protein expression of TNF-α in ventricular cardiomyocytes and restored the I_{to} function by elevating its channel components. Another possible mechanism involved in the effect of TNF-α on APD prolongation could be that this cytokine induces alterations in $I_{Ca,\,L}$. However, previous study in our lab indicated that $I_{Ca,L}$ density in rat ventricular myocytes from fistula rats was comparable to that from control rats.[26] Similar results of I_{CaL} density have been obtained in rat ventricular myocytes in the presence of 10-25ng/ml TNF-α.[165]

In summary, out data demonstrated that downregulated expression of I_{to} isoforms Kv4.2, Kv4.3 and KChIP2 may contribute to the prolongation of APD and the lengthened QT interval in the heart of rats with the volume-overload heart failure. Administration of APN could restore the I_{to} function and the duration of AP in the ventricular myocytes by suppressing the protein levels of TNF-α, which may prevent or attenuate the electrophysiological remodeling due to cardiac volume overload.

Figure Legend

Figure 3-1 Action potential duration (APD) in ventricular myocytes following 10-week fistula **a** representative action potential waveforms recorded from Control (CTL), Control+Ad-APN (CTL+Ad-APN), Fistula and Fistula+Ad-APN ventricular myocytes; **b** analysis of APD at 50% repolarization in ventricular myocytes isolated from four groups. Results were presented as mean ± SEM for Control (n=6), Control+Ad-APN (n=7), Fistula (n=10) and Fistula+Ad-APN (n=8). * $P<0.05$ compared with Control. # $P<0.05$ compared with Fistula+Ad-APN.

Figure 3-2 The QT interval on the surface electrocardiogram (ECG). Results were presented as mean ± SEM for Control (n=6), Control+Ad-APN (n=7), Fistula (n=10) and Fistula+Ad-APN (n=8) groups. * $P<0.05$ compared with Control. # $P<0.05$ compared with Fistula+Ad-APN.

Figure 3-3 Transient outward potassium current (I_{to}) current amplitude and density ventricular myocytes at 10 weeks post-fistula **a** represented the whole-cell I_{to} currents recorded from Control (CTL), Control+Ad-APN (CTL+Ad-APN), Fistula and Fistula+Ad-APN ventricular myocytes after exposure to 40 mM of tetraethylammonium (TEA); **b** Mean current-voltage relationships were shown for peak I_{to} current density. Results were presented as mean ± SEM for Control (n=6), Control+Ad-APN (n=7), Fistula (n=10) and Fistula+Ad-APN (n=8). * $P<0.05$ compared with Control. # $P<0.05$ compared with Fistula+Ad-APN.

Figure 3-4 Protein levels of transient outward potassium channel (I_{to}) components in ventricular myocytes at 10 weeks post-fistula **a and b** representative protein expression of Kv4.3 on the membrane and in the cytosol from different groups; **c and d** representative protein expression of Kv4.2 on the membrane and in the cytosol from

different groups; **e and f** representative protein expression of KChIP2 on the membrane and in the cytosol. Ponceau S or GAPDH were used to normalize protein signals. Results were presented as mean ± SEM for Control (n=6), Control+Ad-APN (n=7), Fistula (n=10) and Fistula+Ad-APN (n=8). * $P<0.05$ compared with Control. # $P<0.05$ compared with Fistula+Ad-APN.

Figure 3-5 Protein levels of tumor necrosis factor-α (TNF-α) in ventricular myocytes at 10 weeks post-fistula **a** representative examples of western blot for TNF-α in ventricular myocytes from different groups; b quantification of protein levels of TNF-α in ventricular myocytes from different groups. GAPDH was used to normalize protein signals. Results were presented as mean ± SEM for Control (n=6), Control+Ad-APN (n=7), Fistula (n=10) and Fistula+Ad-APN (n=8). * $P<0.05$ compared with Control. # $P<0.05$ compared with Fistula+Ad-APN.

Figure 3-1 Action potential duration (APD) in ventricular myocytes following 10-week fistula

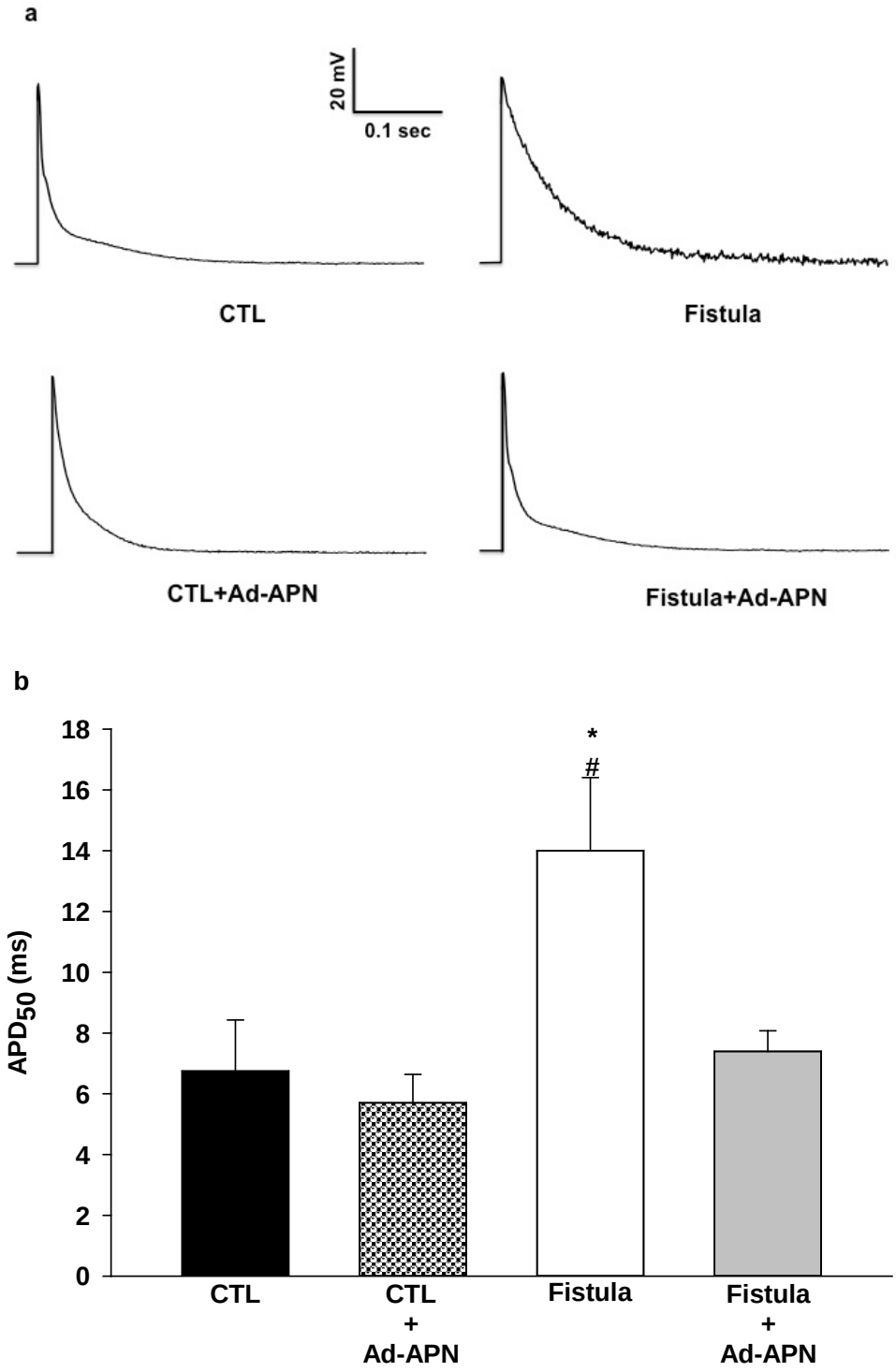
a
20 mV
0.1 sec
CTL
Fistula
CTL+Ad-APN
Fistula+Ad-APN
b
APD50 (ms)
0
2
4
6
8
10
12
14
16
18
*
#
CTL
CTL + Ad-APN
Fistula
Fistula + Ad-APN

Figure 3-2 The QT interval on the surface electrocardiogram (ECG) at 10 weeks post-fistula

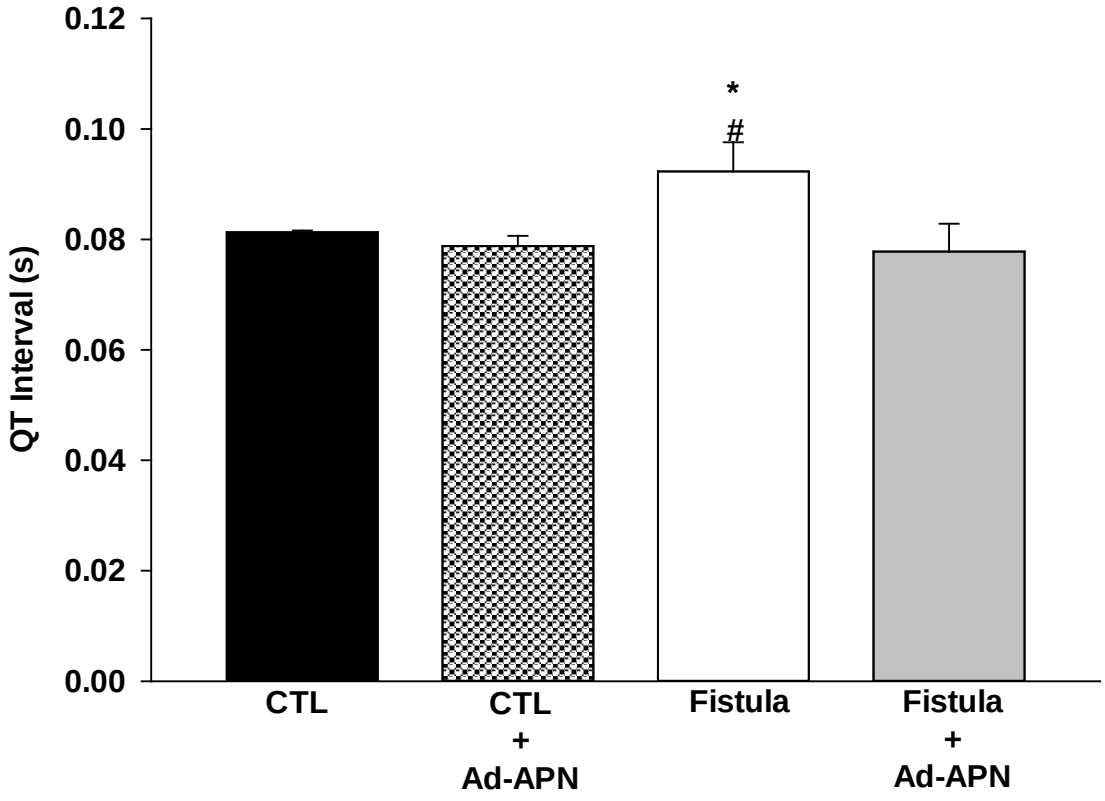
0.12
0.10
0.08
0.06
0.04
0.02
0.00
QT Interval (s)
*
#
CTL
CTL + Ad-APN
Fistula
Fistula + Ad-APN

Figure 3-3 Transient outward potassium current (I_{to}) current amplitude and density ventricular myocytes at 10 weeks post-fistula

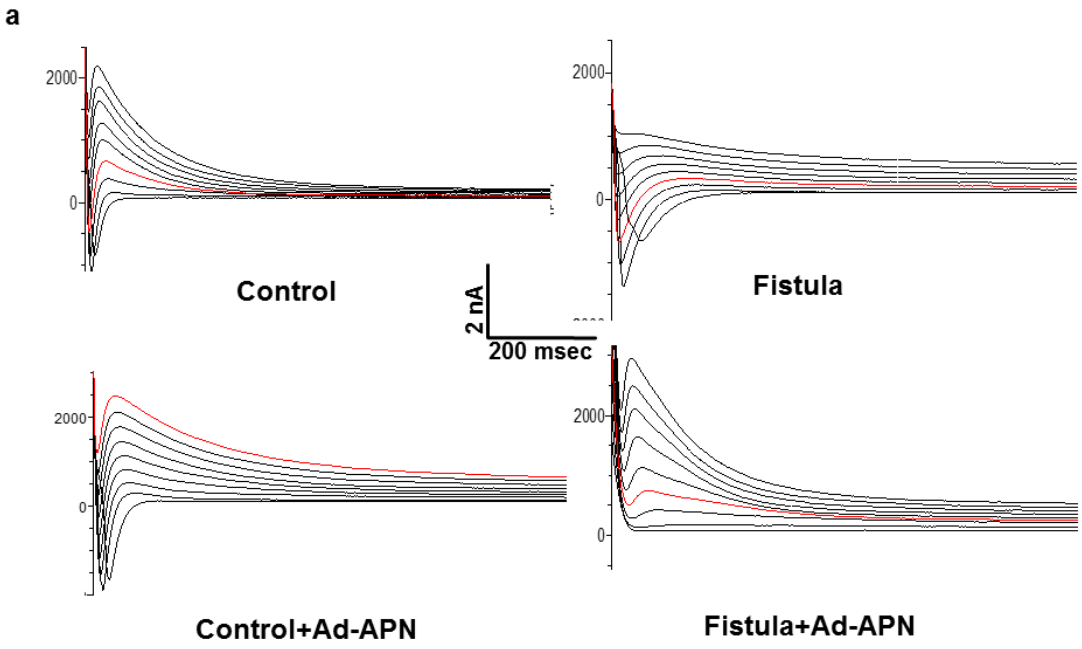
a
2000
0
Control
2 nA
200 msec
Fistula
Control+Ad-APN
Fistula+Ad-APN

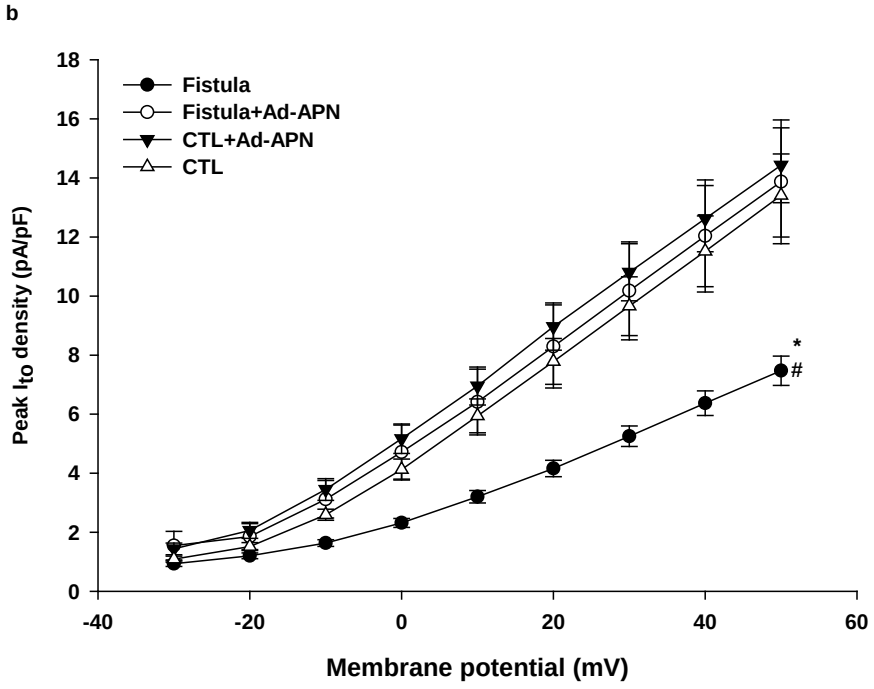
b
Fistula
Fistula+Ad-APN
CTL+Ad-APN
CTL
Peak I_{to} density (pA/pF)
Membrane potential (mV)
*
#

Figure 3-4 Protein levels of transient outward potassium channel (I_{to}) components in ventricular myocytes at 10 weeks post-fistula

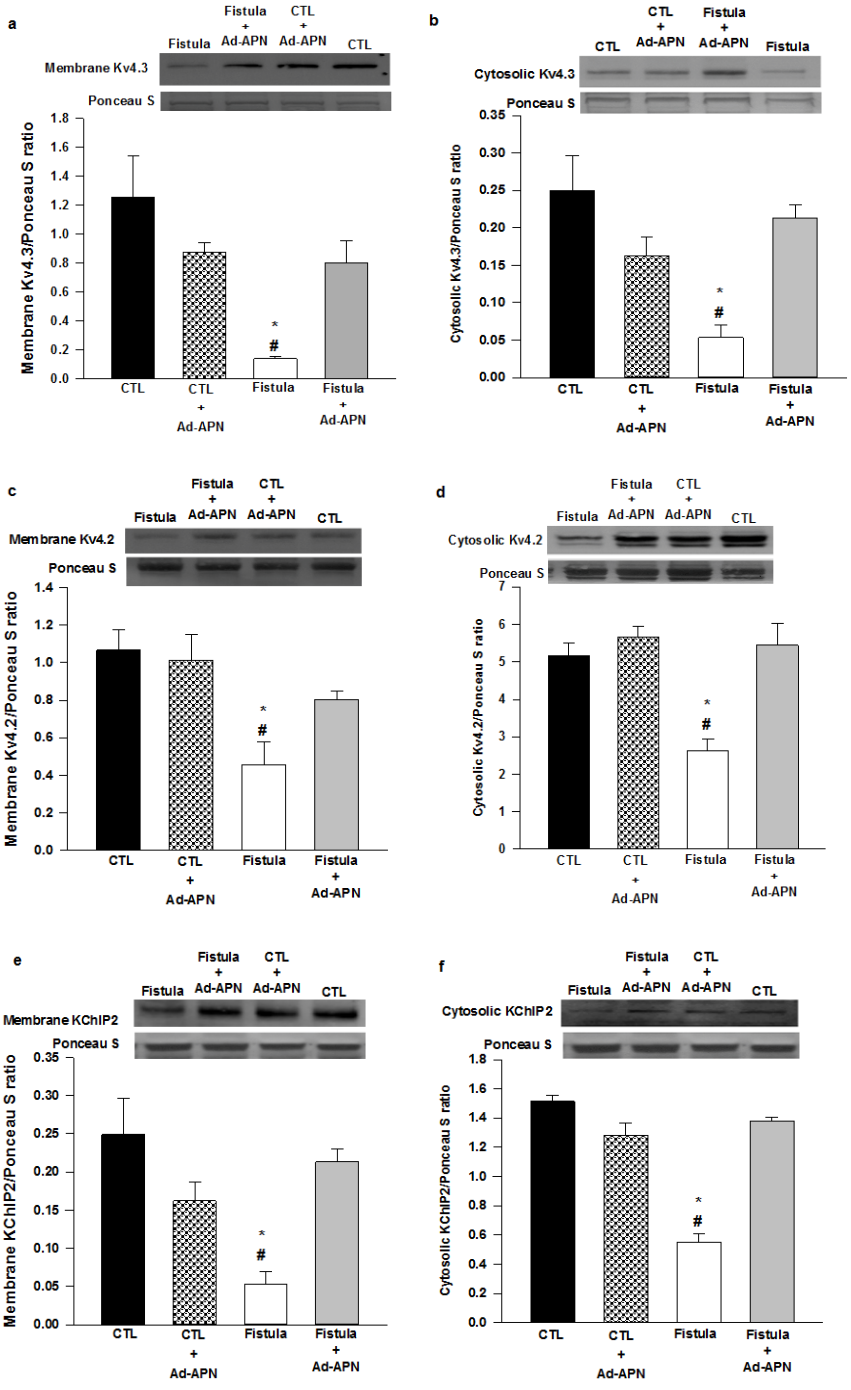
a
Fistula
Fistula + Ad-APN
CTL + Ad-APN
CTL
Membrane Kv4.3
Ponceau S
Membrane Kv4.3/Ponceau S ratio
CTL
CTL + Ad-APN
Fistula
Fistula + Ad-APN
b
Cytosolic Kv4.3
Cytosolic Kv4.3/Ponceau S ratio
c
Membrane Kv4.2
Membrane Kv4.2/Ponceau S ratio
d
Cytosolic Kv4.2
Cytosolic Kv4.2/Ponceau S ratio
e
Membrane KChIP2
Membrane KChIP2/Ponceau S ratio
f
Cytosolic KChIP2
Cytosolic KChIP2/Ponceau S ratio

Figure 3-5 Protein levels of tumor necrosis factor-α (TNF-α) in ventricular myocytes at 10 weeks post-fistula

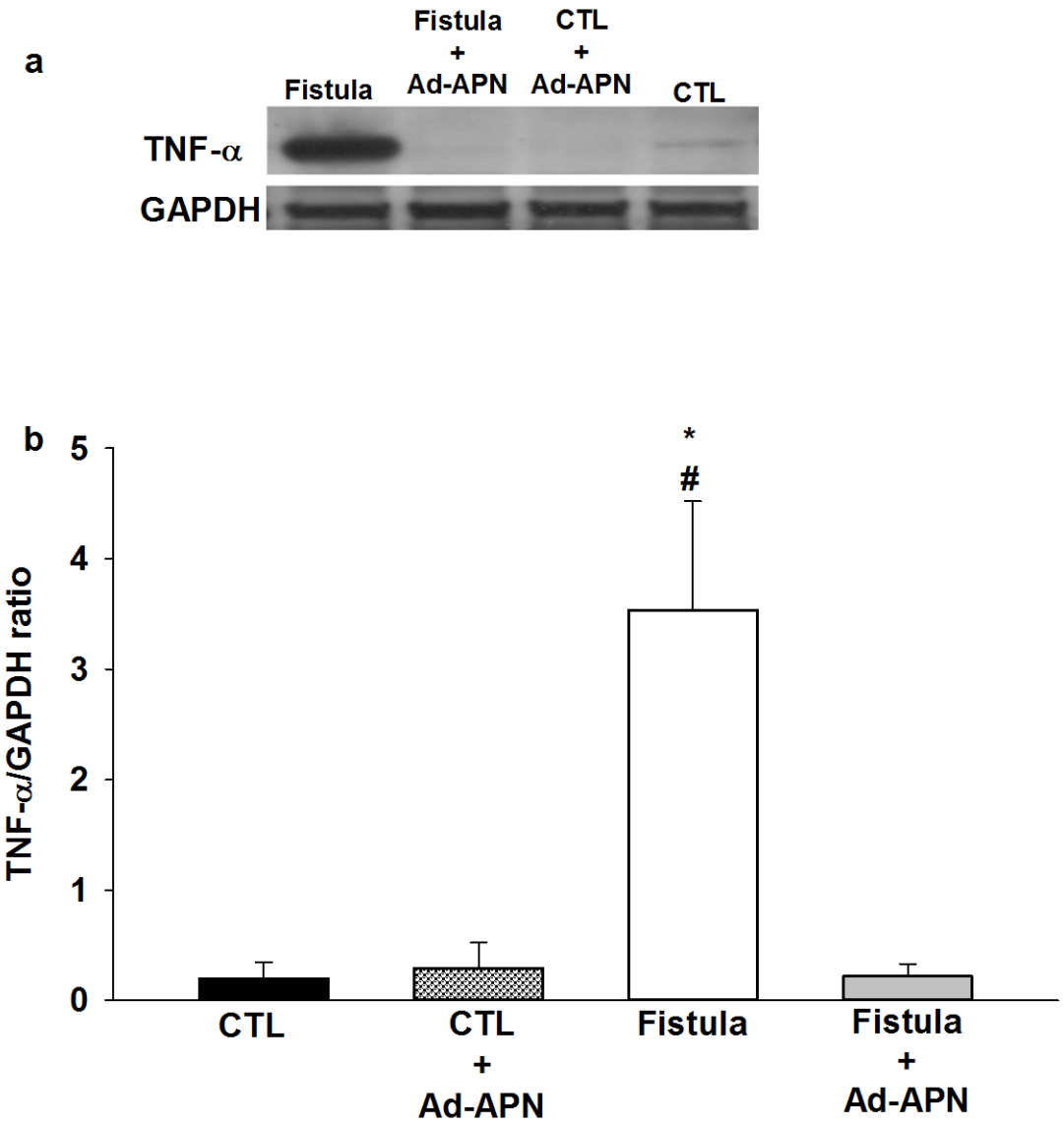
a
Fistula
Fistula + Ad-APN
CTL + Ad-APN
CTL
TNF-α
GAPDH
b
TNF-α/GAPDH ratio
0
1
2
3
4
5
*
#
CTL
CTL + Ad-APN
Fistula
Fistula + Ad-APN

Conclusion and Future Prospective

In the first study, our data indicated a progressive reduction of serum APN levels during the development of volume-overload heart failure. Additionally, APN and AdipoRs protein levels were decreased, and AMPK activity was reduced in ventricular myocytes following 12-week fistula. Consistent with these, myocytes exhibited significant depression in cell shortening and intracellular Ca^{2+} transient. *In vivo* supplementation of APN significantly increased APN serum levels, and prevented the depression of myocyte contractile performance following 12-week fistula. Moreover, *in vitro* treatment with APN also significantly improved myocyte contractility and intracellular Ca^{2+} transient from 12-week fistula rat. These results demonstrate a positive correlation of APN reduction and ventricular contractile dysfunction due to volume overload.

In the second study, our results showed that the duration of action potential was prolonged in ventricular myocytes following 10-week fistula, which, in turn, was reflected by the lengthened QT interval on the surface ECG. The prolongation of action potential duration was correlated with a depression of I_{to} function as well as a decrease of I_{to} channel components expression in ventricular myocytes at 10 weeks post-fistula. In addition, the protein level of tumor necrosis factor-α (TNF-α) was significantly increased

in ventricular myocytes at 10 weeks post-fistula. However, supplementation of Ad-APN increased the protein levels of I_{to} channel components and reversed I_{to} function in ventricular myocytes following 10-week fistula. This further restored the duration of action potential and the QT interval on the ECG back to the normal. In addition, the administration of Ad-APN significantly reduced the protein level of TNF-α in ventricular myocytes even following 10-week fistula. These results indicated that APN might prevent the volume overload-induced ventricular electrophysiological remodeling via a decreased production of TNF-α in ventricular myocytes.

These two studies confirmed the protective effect of APN in volume overload-induced heart failure. Further studies to identify the APN-mediated signaling pathways will provide important links in understanding the molecular mechanisms of APN in protecting the heart against volume overload-induced cardiac injury.

Reference

1. Goktepe S, Abilez OJ, Parker KK, Kuhl E. A multiscale model for eccentric and concentric cardiac growth through sarcomerogenesis. *J Theor Biol* 2010;**265**:433-442. doi:10.1016/j.jtbi.2010.04.023
2. Go AS, Mozaffarian D, Roger VL, Benjamin EJ, Berry JD, Blaha MJ, Dai S, Ford ES, Fox CS, Franco S, Fullerton HJ, Gillespie C, Hailpern SM, Heit JA, Howard VJ, Huffman MD, Judd SE, Kissela BM, Kittner SJ, Lackland DT, Lichtman JH, Lisabeth LD, Mackey RH, Magid DJ, Marcus GM, Marelli A, Matchar DB, McGuire DK, Mohler ER, 3rd, Moy CS, Mussolino ME, Neumar RW, Nichol G, Pandey DK, Paynter NP, Reeves MJ, Sorlie PD, Stein J, Towfighi A, Turan TN, Virani SS, Wong ND, Woo D, Turner MB. Heart disease and stroke statistics--2014 update: a report from the American Heart Association. *Circulation* 2014;**129**:e28-e292. doi:10.1161/01.cir.0000441139.02102.80
3. Cantor EJ, Babick AP, Vasanji Z, Dhalla NS, Netticadan T. A comparative serial echocardiographic analysis of cardiac structure and function in rats subjected to pressure or volume overload. *J Mol Cell Cardiol* 2005;**38**:777-786. doi:10.1016/j.yjmcc.2005.02.012
4. Mann DL. Basic mechanisms of left ventricular remodeling: the contribution of wall stress. *J Card Fail* 2004;**10**:S202-206. doi:doi:10.1016/j.cardfail.2004.09.008

5. Frey N, Katus HA, Olson EN, Hill JA. Hypertrophy of the heart: a new therapeutic target? *Circulation* 2004;**109**:1580-1589. doi:10.1161/01.CIR.0000120390.68287.BB

6. Dickhout JG, Carlisle RE, Austin RC. Interrelationship between cardiac hypertrophy, heart failure, and chronic kidney disease: endoplasmic reticulum stress as a mediator of pathogenesis. *Circ Res* 2011;**108**:629-642. doi:10.1161/circresaha.110.226803

7. Bonow RO, Carabello B, de Leon AC, Jr., Edmunds LH, Jr., Fedderly BJ, Freed MD, Gaasch WH, McKay CR, Nishimura RA, O'Gara PT, O'Rourke RA, Rahimtoola SH, Ritchie JL, Cheitlin MD, Eagle KA, Gardner TJ, Garson A, Jr., Gibbons RJ, Russell RO, Ryan TJ, Smith SC, Jr. Guidelines for the management of patients with valvular heart disease: executive summary. A report of the American College of Cardiology/American Heart Association Task Force on Practice Guidelines (Committee on Management of Patients with Valvular Heart Disease). *Circulation* 1998;**98**:1949-1984. doi:10.1161/01.CIR.98.18.1949

8. Mann DL, Bristow MR. Mechanisms and models in heart failure: the biomechanical model and beyond. *Circulation* 2005;**111**:2837-2849. doi:10.1161/circulationaha.104.500546

9. Haluzik M, Parizkova J, Haluzik MM. Adiponectin and Its Role in the Obesity-Induced Insulin Resistance and Related Complications. *Physiol Res* 2004;**53**:123-129.

10. Fang X, Sweeney G. Mechanisms regulating energy metabolism by adiponectin in obesity and diabetes. *Biochem Soc Trans* 2006;**34**:798-801. doi:10.1042/BST0340798

11. Beltowski J, Jamroz-Wisniewska A, Widomska S. Adiponectin and its role in cardiovascular diseases. *Cardiovasc Hematol Disord Drug Targets* 2008;**8**:7-46. doi:10.2174/187152908783884920

12. Skurk C, Wittchen F, Suckau L, Witt H, Noutsias M, Fechner H, Schultheiss HP, Poller W. Description of a local cardiac adiponectin system and its deregulation in dilated cardiomyopathy. *Eur Heart J* 2008;**29**:1168-1180. doi:10.1093/eurheartj/ehn136

13. Wang Y, Lau WB, Gao E, Tao L, Yuan Y, Li R, Wang X, Koch WJ, Ma XL. Cardiomyocyte-derived adiponectin is biologically active in protecting against myocardial ischemia-reperfusion injury. *Am J Physiol Endocrinol Metab* 2010;**298**:E663-670. doi:10.1152/ajpendo.00663.2009.

14. Dadson K, Liu Y, Sweeney G. Adiponectin action: a combination of endocrine and autocrine/paracrine effects. *Front Endocrinol (Lausanne)* 2011;**2**:62. doi:10.3389/fendo.2011.00062

15. Caselli C, D'Amico A, Cabiati M, Prescimone T, Del Ry S, Giannessi D. Back to the heart: The protective role of adiponectin. *Pharmacol Res* 2014;**82c**:9-20. doi:10.1016/j.phrs.2014.03.003

16. Ouchi N, Shibata R, Walsh K. Cardioprotection by adiponectin. *Trends Cardiovasc Med* 2006;**16**:141-146. doi:10.1016/j.tcm.2006.03.001

17. Sadoshima J, Izumo S. The cellular and molecular response of cardiac myocytes to mechanical stress. *Annu Rev Physiol* 1997;**59**:551-571. doi:10.1146/annurev.physiol.59.1.551

18. Lorell BH, Carabello BA. Left Ventricular Hypertrophy : Pathogenesis, Detection, and Prognosis. *Circulation* 2000;**102**:470-479. doi:10.1161/01.cir.102.4.470

19. Ahuja P, Sdek P, MacLellan WR. Cardiac myocyte cell cycle control in development, disease, and regeneration. *Physiol Rev* 2007;**87**:521-544. doi:10.1152/physrev.00032.2006

20. Grossman W, Jones D, McLaurin LP. Wall stress and patterns of hypertrophy in the human left ventricle. *J Clin Invest* 1975;**56**:56-64. doi:10.1172/jci108079

21. Imamura T, McDermott PJ, Kent RL, Nagatsu M, Cooper Gt, Carabello BA. Acute changes in myosin heavy chain synthesis rate in pressure versus volume overload. *Circ Res* 1994;**75**:418-425. doi:10.1161/01.RES.75.3.418

22. Linke WA. Sense and stretchability: the role of titin and titin-associated proteins in myocardial stress-sensing and mechanical dysfunction. *Cardiovasc Res* 2008;**77**:637-648. doi:10.1016/j.cardiores.2007.03.029

23. Kehat I, Molkentin JD. Extracellular signal-regulated kinase 1/2 (ERK1/2) signaling in cardiac hypertrophy. *Ann N Y Acad Sci* 2010;**1188**:96-102. doi:10.1111/j.1749-6632.2009.05088.x

24. Kehat I, Davis J, Tiburcy M, Accornero F, Saba-El-Leil MK, Maillet M, York AJ, Lorenz JN, Zimmermann WH, Meloche S, Molkentin JD. Extracellular signal-regulated kinases 1 and 2 regulate the balance between eccentric and concentric cardiac growth. *Circ Res* 2011;**108**:176-183. doi:10.1161/circresaha.110.231514

25. Toischer K, Rokita AG, Unsold B, Zhu W, Kararigas G, Sossalla S, Reuter SP, Becker A, Teucher N, Seidler T, Grebe C, Preuss L, Gupta SN, Schmidt K, Lehnart SE, Kruger M, Linke WA, Backs J, Regitz-Zagrosek V, Schafer K, Field LJ, Maier LS, Hasenfuss G. Differential cardiac remodeling in preload versus afterload. *Circulation* 2010;**122**:993-1003. doi:10.1161/circulationaha.110.943431

26. Ding YF, Brower GL, Zhong Q, Murray D, Holland M, Janicki JS, Zhong J. Defective intracellular Ca2+ homeostasis contributes to myocyte dysfunction during ventricular remodelling induced by chronic volume overload in rats. *Clin Exp Pharmacol Physiol* 2008;**35**:827-835. doi:10.1111/j.1440-1681.2008.04923.x

27. Gladden JD, Zelickson BR, Guichard J, Ahmed MI, Yancey DM, Ballinger SW, Shanmugam M, Babu GJ, Johnson MS, Darley-Usmar VM, Dell'italia LJ. Xanthine Oxidase Inhibition Preserves Left Ventricular Systolic but not Diastolic Function in Cardiac Volume Overload. *Am J Physiol Heart Circ Physiol* 2013;**305**:H1440-1450. doi:10.1152/ajpheart.00007.2013

28. Carabello BA, Zile MR, Tanaka R, Cooper Gt. Left ventricular hypertrophy due to volume overload versus pressure overload. *Am J Physiol* 1992;**263**:H1137-1144.

29. Riquelme CA, Magida JA, Harrison BC, Wall CE, Marr TG, Secor SM, Leinwand LA. Fatty acids identified in the Burmese python promote beneficial cardiac growth. *Science* 2011;**334**:528-531. doi:10.1126/science.1210558

30. Harrison BC, Roberts CR, Hood DB, Sweeney M, Gould JM, Bush EW, McKinsey TA. The CRM1 nuclear export receptor controls pathological cardiac gene expression. *Mol Cell Biol* 2004;**24**:10636-10649. doi:10.1128/mcb.24.24.10636-10649.2004

31. Bernardo BC, Weeks KL, Pretorius L, McMullen JR. Molecular distinction between physiological and pathological cardiac hypertrophy: experimental findings and therapeutic strategies. *Pharmacol Ther* 2010;**128**:191-227. doi:10.1016/j.pharmthera.2010.04.005

32. McMullen JR, Jennings GL. Differences between pathological and physiological cardiac hypertrophy: novel therapeutic strategies to treat heart failure. *Clin Exp Pharmacol Physiol* 2007;**34**:255-262. doi:10.1111/j.1440-1681.2007.04585.x

33. Levy D, Garrison RJ, Savage DD, Kannel WB, Castelli WP. Prognostic implications of echocardiographically determined left ventricular mass in the Framingham Heart Study. *N Engl J Med* 1990;**322**:1561-1566. doi:10.1056/nejm199005313222203

34. Rayner J, Coffey S, Newton J, Prendergast BD. Aortic valve disease. *Int J Clin Pract* 2014;**68**:1209-1215. doi:10.1111/ijcp.12471

35. Nishimura RA. Cardiology patient pages. Aortic valve disease. *Circulation* 2002;**106**:770-772. doi:10.1161/01.CIR.0000027621.26167.5E

36. Melenovsky V. Cardiac Adaptation to Volume Overload. *Cardiac Adaptations* 2013;**4**:167-199. doi:10.1007/978-1-4614-5203-4_9

37. Stern AB, Klemmer PJ. High-output heart failure secondary to arteriovenous fistula. *Hemodial Int* 2011. doi:10.1111/j.1542-4758.2010.00518.x

38. Hall JE. Guyton and Hall Textbook of Medical Physiology. 2013.

39. Naito Y, Tsujino T, Matsumoto M, Sakoda T, Ohyanagi M, Masuyama T. Adaptive response of the heart to long-term anemia induced by iron deficiency. *Am J Physiol Heart Circ Physiol* 2009;**296**:H585-593. doi:10.1152/ajpheart.00463.2008

40. Anand IS, Florea VG. High Output Cardiac Failure. *Curr Treat Options Cardiovasc Med* 2001;**3**:151-159.

41. Chrysant SG. Current status of dual Renin Angiotensin aldosterone system blockade for the treatment of cardiovascular diseases. *Am J Cardiol* 2010;**105**:849-852. doi:10.1016/j.amjcard.2009.11.044

42. Ferrario CM, Strawn WB. Role of the renin-angiotensin-aldosterone system and proinflammatory mediators in cardiovascular disease. *Am J Cardiol* 2006;**98**:121-128. doi:10.1016/j.amjcard.2006.01.059

43. Ryan TD, Rothstein EC, Aban I, Tallaj JA, Husain A, Lucchesi PA, Dell'Italia LJ. Left ventricular eccentric remodeling and matrix loss are mediated by bradykinin

and precede cardiomyocyte elongation in rats with volume overload. *J Am Coll Cardiol* 2007;**49**:811-821. doi:10.1016/j.jacc.2006.06.083

44. Shin J, Johnson JA. Pharmacogenetics of beta-blockers. *Pharmacotherapy* 2007;**27**:874-887. doi:10.1592/phco.27.6.874

45. Bavishi C, Chatterjee S, Ather S, Patel D, Messerli FH. Beta-blockers in heart failure with preserved ejection fraction: a meta-analysis. *Heart Fail Rev* 2014. doi:10.1007/s10741-014-9453-8

46. Barrese V, Taglialatela M. New advances in beta-blocker therapy in heart failure. *Front Physiol* 2013;**4**:323. doi:10.3389/fphys.2013.00323

47. Borer JS, Bonow RO. Contemporary approach to aortic and mitral regurgitation. *Circulation* 2003;**108**:2432-2438. doi:10.1161/01.CIR.0000096400.00562.A3

48. Bonow RO. Chronic mitral regurgitation and aortic regurgitation: have indications for surgery changed? *J Am Coll Cardiol* 2013;**61**:693-701. doi:10.1016/j.jacc.2012.08.1025

49. Melenovsky V, Benes J, Skaroupkova P, Sedmera D, Strnad H, Kolar M, Vlcek C, Petrak J, Benes J, Jr., Papousek F, Oliyarnyk O, Kazdova L, Cervenka L. Metabolic characterization of volume overload heart failure due to aorto-caval fistula in rats. *Mol Cell Biochem* 2011;**354**:83-96. doi:10.1007/s11010-011-0808-3

50. Brower GL, Henegar JR, Janicki JS. Temporal evaluation of left ventricular remodeling and function in rats with chronic volume overload. *Am J Physiol* 1996;**271**:H2071-2078.

51. Janicki JS, Brower GL, Gardner JD, Chancey AL, Stewart JA, Jr. The dynamic interaction between matrix metalloproteinase activity and adverse myocardial remodeling. *Heart Fail Rev* 2004;**9**:33-42. doi:10.1023/B:HREV.0000011392.03037.7e

52. Brower GL, Janicki JS. Contribution of ventricular remodeling to pathogenesis of heart failure in rats. *Am J Physiol Heart Circ Physiol* 2001;**280**:H674-683.

53. Altin SE, Schulze PC. Metabolism of the right ventricle and the response to hypertrophy and failure. *Prog Cardiovasc Dis* 2012;**55**:229-233. doi:10.1016/j.pcad.2012.07.010

54. Akhmedov AT, Rybin V, Marin-Garcia J. Mitochondrial oxidative metabolism and uncoupling proteins in the failing heart. *Heart Fail Rev* 2014. doi:10.1007/s10741-014-9457-4

55. Aiba T, Tomaselli GF. Electrical remodeling in the failing heart. *Curr Opin Cardiol* 2010;**25**:29-36. doi:10.1097/HCO.0b013e328333d3d6

56. Cutler MJ, Jeyaraj D, Rosenbaum DS. Cardiac electrical remodeling in health and disease. *Trends Pharmacol Sci* 2011;**32**:174-180. doi:10.1016/j.tips.2010.12.001

57. de Git KC, de Boer TP, Vos MA, van der Heyden MA. Cardiac ion channel trafficking defects and drugs. *Pharmacol Ther* 2013;**139**:24-31. doi:10.1016/j.pharmthera.2013.03.008

58. Harkcom WT, Abbott GW. Emerging concepts in the pharmacogenomics of arrhythmias: ion channel trafficking. *Expert Rev Cardiovasc Ther* 2010;**8**:1161-1173. doi:10.1586/erc.10.89

59. Wang Y, Hill JA. Electrophysiological remodeling in heart failure. *J Mol Cell Cardiol* 2010;**48**:619-632. doi:10.1016/j.yjmcc.2010.01.009

60. Jeyaraj D, Wan X, Ficker E, Stelzer JE, Deschenes I, Liu H, Wilson LD, Decker KF, Said TH, Jain MK, Rudy Y, Rosenbaum DS. Ionic bases for electrical remodeling of the canine cardiac ventricle. *Am J Physiol Heart Circ Physiol* 2013;**305**:H410-419. doi:10.1152/ajpheart.00213.2013

61. Lopez-Izquierdo A, Pereira RO, Wende AR, Punske BB, Abel ED, Tristani-Firouzi M. The absence of insulin signaling in the heart induces changes in potassium channel expression and ventricular repolarization. *Am J Physiol Heart Circ Physiol* 2014;**306**:H747-754. doi:10.1152/ajpheart.00849.2013

62. Sato T, Kobayashi T, Kuno A, Miki T, Tanno M, Kouzu H, Itoh T, Ishikawa S, Kojima T, Miura T, Tohse N. Type 2 diabetes induces subendocardium-predominant reduction in transient outward K+ current with downregulation of Kv4.2 and KChIP2. *Am J Physiol Heart Circ Physiol* 2014;**306**:H1054-1065. doi:10.1152/ajpheart.00414.2013

63. Briston SJ, Caldwell JL, Horn MA, Clarke JD, Richards MA, Greensmith DJ, Graham HK, Hall MC, Eisner DA, Dibb KM, Trafford AW. Impaired beta-adrenergic responsiveness accentuates dysfunctional excitation-contraction

coupling in an ovine model of tachypacing-induced heart failure. *J Physiol* 2011;**589**:1367-1382. doi:10.1113/jphysiol.2010.203984

64. Wang Z, Kutschke W, Richardson KE, Karimi M, Hill JA. Electrical remodeling in pressure-overload cardiac hypertrophy: role of calcineurin. *Circulation* 2001;**104**:1657-1663. doi:10.1161/hc3901.095766

65. Undrovinas A, Maltsev VA. Late sodium current is a new therapeutic target to improve contractility and rhythm in failing heart. *Cardiovasc Hematol Agents Med Chem* 2008;**6**:348-359. doi:10.2174/187152508785909447

66. Stumvoll M, Tschritter O, Fritsche A, Staiger H, Renn W, Weisser M, Machicao F, Haring H. Association of the T-G polymorphism in adiponectin (exon 2) with obesity and insulin sensitivity: interaction with family history of type 2 diabetes. *Diabetes* 2002;**51**:37-41. doi:10.2337/diabetes.51.1.37

67. Wang Y, Lam KS, Yau MH, Xu A. Post-translational modifications of adiponectin: mechanisms and functional implications. *Biochem J* 2008;**409**:623-633. doi:10.1042/BJ20071492

68. Hug C, Lodish HF. The role of the adipocyte hormone adiponectin in cardiovascular disease. *Curr Opin Pharmacol* 2005;**5**:129-134. doi:10.1016/j.coph.2005.01.001

69. Shapiro L, Scherer PE. The crystal structure of a complement-1q family protein suggests an evolutionary link to tumor necrosis factor. *Curr Biol* 1998;**8**:335-338. doi:10.1016/S0960-9822(98)70133-2

70. Hui X, Lam KS, Vanhoutte PM, Xu A. Adiponectin and cardiovascular health: an update. *Br J Pharmacol* 2012;**165**:574-590. doi:10.1111/j.1476-5381.2011.01395.x

71. Tsao TS, Tomas E, Murrey HE, Hug C, Lee DH, Ruderman NB, Heuser JE, Lodish HF. Role of disulfide bonds in Acrp30/adiponectin structure and signaling specificity. Different oligomers activate different signal transduction pathways. *J Biol Chem* 2003;**278**:50810-50817. doi:10.1074/jbc.M309469200

72. Wang ZV, Schraw TD, Kim JY, Khan T, Rajala MW, Follenzi A, Scherer PE. Secretion of the adipocyte-specific secretory protein adiponectin critically depends on thiol-mediated protein retention. *Mol Cell Biol* 2007;**27**:3716-3731. doi:10.1128/MCB.00931-06

73. Liu M, Zhou L, Xu A, Lam KS, Wetzel MD, Xiang R, Zhang J, Xin X, Dong LQ, Liu F. A disulfide-bond A oxidoreductase-like protein (DsbA-L) regulates adiponectin multimerization. *Proc Natl Acad Sci U S A* 2008;**105**:18302-18307. doi:10.1073/pnas.0806341105

74. Waki H, Yamauchi T, Kamon J, Kita S, Ito Y, Hada Y, Uchida S, Tsuchida A, Takekawa S, Kadowaki T. Generation of globular fragment of adiponectin by leukocyte elastase secreted by monocytic cell line THP-1. *Endocrinology* 2005;**146**:790-796. doi:10.1210/en.2004-1096

75. Fruebis J, Tsao TS, Javorschi S, Ebbets-Reed D, Erickson MR, Yen FT, Bihain BE, Lodish HF. Proteolytic cleavage product of 30-kDa adipocyte complement-

related protein increases fatty acid oxidation in muscle and causes weight loss in mice. *Proc Natl Acad Sci U S A* 2001;**98**:2005-2010. doi:10.1073/pnas.041591798

76. Pajvani UB, Du X, Combs TP, Berg AH, Rajala MW, Schulthess T, Engel J, Brownlee M, Scherer PE. Structure-function studies of the adipocyte-secreted hormone Acrp30/adiponectin. Implications fpr metabolic regulation and bioactivity. *J Biol Chem* 2003;**278**:9073-9085. doi:10.1074/jbc.M207198200

77. Yamauchi T, Kamon J, Ito Y, Tsuchida A, Yokomizo T, Kita S, Sugiyama T, Miyagishi M, Hara K, Tsunoda M, Murakami K, Ohteki T, Uchida S, Takekawa S, Waki H, Tsuno NH, Shibata Y, Terauchi Y, Froguel P, Tobe K, Koyasu S, Taira K, Kitamura T, Shimizu T, Nagai R, Kadokami T. Cloning of adiponectin receptors that mediate antidiabetic metabolic effects. *Nature* 2003;**423**:762-769. doi:10.1038/nature01683

78. Xu A, Vanhoutte PM. Adiponectin and adipocyte fatty acid binding protein in the pathogenesis of cardiovascular disease. *Am J Physiol Heart Circ Physiol* 2012;**302**:H1231-1240. doi:10.1152/ajpheart.00765.2011

79. Fujioka D, Kawabata K, Saito Y, Kobayashi T, Nakamura T, Takano H, Obata JE, Kitta Y, Umetani K, Kugiyama K. Role of adiponectin receptors in endothelin-induced cellular hypertrophy in cultured cardiomyocytes and their expression in infarcted heart. *Am J Physiol Heart Circ Physiol* 2006;**290**:H2409-2416. doi:110.1152/ajpheart.00987.2005

80. Pineiro R, Iglesias MJ, Gallego R, Raghay K, Eiras S, Rubio J, Dieguez C, Gualillo O, Gonzalez-Juanatey JR, Lago F. Adiponectin is synthesized and secreted by human and murine cardiomyocytes. *FEBS Lett* 2005;**579**:5163-5169. doi:10.1016/j.febslet.2005.07.098

81. Tsuchida A, Yamauchi T, Ito Y, Hada Y, Maki T, Takekawa S, Kamon J, Kobayashi M, Suzuki R, Hara K, Kubota N, Terauchi Y, Froguel P, Nakae J, Kasuga M, Accili D, Tobe K, Ueki K, Nagai R, Kadowaki T. Insulin/Foxo1 pathway regulates expression levels of adiponectin receptors and adiponectin sensitivity. *J Biol Chem* 2004;**279**:30817-30822. doi:10.1074/jbc.M402367200

82. Wang C, Xin X, Xiang R, Ramos FJ, Liu M, Lee HJ, Chen H, Mao X, Kikani CK, Liu F, Dong LQ. Yin-Yang regulation of adiponectin signaling by APPL isoforms in muscle cells. *J Biol Chem* 2009;**284**:31608-31615. doi:10.1074/jbc.M109.010355

83. Mao X, Kikani CK, Riojas RA, Langlais P, Wang L, Ramos FJ, Fang Q, Christ-Roberts CY, Hong JY, Kim RY, Liu F, Dong LQ. APPL1 binds to adiponectin receptors and mediates adiponectin signalling and function. *Nat Cell Biol* 2006;**8**:516-523. doi:10.1038/ncb1404

84. Fang X, Palanivel R, Cresser J, Schram K, Ganguly R, Thong FS, Tuinei J, Xu A, Abel ED, Sweeney G. An APPL1-AMPK signaling axis mediates beneficial metabolic effects of adiponectin in the heart. *Am J Physiol Endocrinol Metab* 2010;**299**:E721-729. doi:10.1152/ajpendo.00086.2010

85. Lizcano JM, Goransson O, Toth R, Deak M, Morrice NA, Boudeau J, Hawley SA, Udd L, Makela TP, Hardie DG, Alessi DR. LKB1 is a master kinase that activates 13 kinases of the AMPK subfamily, including MARK/PAR-1. *EMBO J* 2004;**23**:833-843. doi:10.1038/sj.emboj.7600110

86. Nagata D, Hirata Y. The role of AMP-activated protein kinase in the cardiovascular system. *Hypertens Res* 2010;**33**:22-28. doi:10.1038/hr.2009.187

87. Wong AK, Howie J, Petrie JR, Lang CC. AMP-activated protein kinase pathway: a potential therapeutic target in cardiometabolic disease. *Clin Sci (Lond)* 2009;**116**:607-620. doi:10.1042/CS20080066

88. Hug C, Wang J, Ahmad NS, Bogan JS, Tsao TS, Lodish HF. T-cadherin is a receptor for hexameric and high-molecular-weight forms of Acrp30/adiponectin. *Proc Natl Acad Sci U S A* 2004;**101**:10308-10313. doi:10.1073/pnas.0403382101

89. Denzel MS, Scimia MC, Zumstein PM, Walsh K, Ruiz-Lozano P, Ranscht B. T-cadherin is critical for adiponectin-mediated cardioprotection in mice. *J Clin Invest* 2010;**120**:4342-4352. doi:10.1172/JCI43464

90. Sam F, Duhaney TA, Sato K, Wilson RM, Ohashi K, Sono-Romanelli S, Higuchi A, De Silva DS, Qin F, Walsh K, Ouchi N. Adiponectin deficiency, diastolic dysfunction, and diastolic heart failure. *Endocrinology* 2010;**151**:322-331. doi:10.1210/en.2009-0806

91. Fu M, Zhou J, Qian J, Jin X, Zhu H, Zhong C, Zou Y, Ge J. Adiponectin through its biphasic serum level is a useful biomarker during transition from diastolic

dysfunction to systolic dysfunction - an experimental study. *Lipids Health Dis* 2012;**11**:106. doi:10.1186/1476-511x-11-106

92. O'Shea KM, Chess DJ, Khairallah RJ, Rastogi S, Hecker PA, Sabbah HN, Walsh K, Stanley WC. Effects of adiponectin deficiency on structural and metabolic remodeling in mice subjected to pressure overload. *Am J Physiol Heart Circ Physiol* 2010;**298**:H1639-1645. doi:10.1152/ajpheart.00957.2009

93. Shimano M, Ouchi N, Shibata R, Ohashi K, Pimentel DR, Murohara T, Walsh K. Adiponectin deficiency exacerbates cardiac dysfunction following pressure overload through disruption of an AMPK-dependent angiogenic response. *J Mol Cell Cardiol* 2010;**49**:210-220. doi:10.1016/j.yjmcc.2010.02.021

94. Tao L, Gao E, Jiao X, Yuan Y, Li S, Christopher TA, Lopez BL, Koch W, Chan L, Goldstein BJ, Ma XL. Adiponectin cardioprotection after myocardial ischemia/reperfusion involves the reduction of oxidative/nitrative stress. *Circulation* 2007;**115**:1408-1416. doi:10.1161/circulationaha.106.666941

95. Shibata R, Sato K, Pimentel DR, Takemura Y, Kihara S, Ohashi K, Funahashi T, Ouchi N, Walsh K. Adiponectin protects against myocardial ischemia-reperfusion injury through AMPK- and COX-2-dependent mechanisms. *Nat Med* 2005;**11**:1096-1103. doi:10.1038/nm1295

96. Dong F, Ren J. Adiponectin improves cardiomyocyte contractile function in db/db diabetic obese mice. *Obesity (Silver Spring)* 2009;**17**:262-268. doi:10.1038/oby.2008.545

97. Dong F, Ren J. Fidarestat improves cardiomyocyte contractile function in db/db diabetic obese mice through a histone deacetylase Sir2-dependent mechanism. *J Hypertens* 2007;**25**:2138-2147. doi:10.1097/HJH.0b013e32828626d1

98. Go AS, Mozaffarian D, Roger VL, Benjamin EJ, Berry JD, Borden WB, Bravata DM, Dai S, Ford ES, Fox CS, Franco S, Fullerton HJ, Gillespie C, Hailpern SM, Heit JA, Howard VJ, Huffman MD, Kissela BM, Kittner SJ, Lackland DT, Lichtman JH, Lisabeth LD, Magid D, Marcus GM, Marelli A, Matchar DB, McGuire DK, Mohler ER, Moy CS, Mussolino ME, Nichol G, Paynter NP, Schreiner PJ, Sorlie PD, Stein J, Turan TN, Virani SS, Wong ND, Woo D, Turner MB, American Heart Association Statistics C, Stroke Statistics S. Heart disease and stroke statistics--2013 update: a report from the American Heart Association. *Circulation* 2013;**127**:e6-e245. doi:10.1161/CIR.0b013e31828124ad

99. Sciarretta S, Sadoshima J. New insights into the molecular phenotype of eccentric hypertrophy. *J Mol Cell Cardiol* 2010;**49**:153-156. doi:10.1016/j.yjmcc.2010.03.018

100. Palanivel R, Fang X, Park M, Eguchi M, Pallan S, De Girolamo S, Liu Y, Wang Y, Xu A, Sweeney G. Globular and full-length forms of adiponectin mediate specific changes in glucose and fatty acid uptake and metabolism in cardiomyocytes. *Cardiovasc Res* 2007;**75**:148-157. doi:10.1016/j.cardiores.2007.04.011

101. Kanda T, Saegusa S, Takahashi T, Sumino H, Morimoto S, Nakahashi T, Iwai K, Matsumoto M. Reduced-energy diet improves survival of obese KKAy mice with

viral myocarditis: induction of cardiac adiponectin expression. *Int J Cardiol* 2007;**119**:310-318. doi:10.1016/j.ijcard.2006.07.181

102. Youn JC, Kim C, Park S, Lee SH, Kang SM, Choi D, Son NH, Shin DJ, Jang Y. Adiponectin and progression of arterial stiffness in hypertensive patients. *Int J Cardiol* 2013;**163**:316-319. doi:10.1016/j.ijcard.2011.06.061

103. Teijeira-Fernandez E, Eiras S, Grigorian-Shamagian L, Fernandez A, Adrio B, Gonzalez-Juanatey JR. Epicardial adipose tissue expression of adiponectin is lower in patients with hypertension. *J Hum Hypertens* 2008;**22**:856-863. doi:10.1038/jhh.2008.75

104. Hashimoto N, Kanda J, Nakamura T, Horie A, Kurosawa H, Hashimoto T, Sato K, Kushida S, Suzuki M, Yano S, Iwai R, Takahashi H, Yoshida S. Association of hypoadiponectinemia in men with early onset of coronary heart disease and multiple coronary artery stenoses. *Metabolism* 2006;**55**:1653-1657. doi:10.1016/j.metabol.2006.08.005

105. Shibata R, Ouchi N, Ito M, Kihara S, Shiojima I, Pimentel DR, Kumada M, Sato K, Schiekofer S, Ohashi K, Funahashi T, Colucci WS, Walsh K. Adiponectin-mediated modulation of hypertrophic signals in the heart. *Nat Med* 2004;**10**:1384-1389. doi:10.1038/nm1137

106. Shibata R, Izumiya Y, Sato K, Papanicolaou K, Kihara S, Colucci WS, Sam F, Ouchi N, Walsh K. Adiponectin protects against the development of systolic

dysfunction following myocardial infarction. *J Mol Cell Cardiol* 2007;**42**:1065-1074. doi:10.1016/j.yjmcc.2007.03.808

107. Ding Y, Zou R, Judd RL, Zhong J. Endothelin-1 receptor blockade prevented the electrophysiological dysfunction in cardiac myocytes of streptozotocin-induced diabetic rats. *Endocrine* 2006;**30**:121-127. doi:10.1385/ENDO:30:1:121

108. Yan W, Zhang H, Liu P, Wang H, Liu J, Gao C, Liu Y, Lian K, Yang L, Sun L, Guo Y, Zhang L, Dong L, Lau WB, Gao E, Gao F, Xiong L, Wang H, Qu Y, Tao L. Impaired mitochondrial biogenesis due to dysfunctional adiponectin-AMPK-PGC-1alpha signaling contributing to increased vulnerability in diabetic heart. *Basic Res Cardiol* 2013;**108**:329. doi:10.1007/s00395-013-0329-1

109. Kehat I, Molkentin JD. Molecular pathways underlying cardiac remodeling during pathophysiological stimulation. *Circulation* 2010;**122**:2727-2735. doi:10.1161/CIRCULATIONAHA.110.942268

110. Rohini A, Agrawal N, Koyani CN, Singh R. Molecular targets and regulators of cardiac hypertrophy. *Pharmacol Res* 2010;**61**:269-280. doi:10.1016/j.phrs.2009.11.012

111. Lee B, Shao J. Adiponectin and energy homeostasis. *Rev Endocr Metab Disord* 2014;**15**:149-156. doi:10.1007/s11154-013-9283-3

112. Arita Y, Kihara S, Ouchi N, Takahashi M, Maeda K, Miyagawa J, Hotta K, Shimomura I, Nakamura T, Miyaoka K, Kuriyama H, Nishida M, Yamashita S, Okubo K, Matsubara K, Muraguchi M, Ohmoto Y, Funahashi T, Matsuzawa Y.

Paradoxical Decrease of an Adipose-Specific Protein, Adiponectin, in Obesity. *Biochem Biophys Res Commun* 1999;**257**:79-83. doi:10.1016/j.bbrc.2012.08.024

113. Hotta K, Funahashi T, Arita Y, Takahashi M, Matsuda M, Okamoto Y, Iwahashi H, Kuriyama H, Ouchi N, Maeda K, Nishida M, Kihara S, Sakai N, Nakajima T, Hasegawa K, Muraguchi M, Ohmoto Y, Nakamura T, Yamashita S, Hanafusa T, Matsuzawa Y. Plasma concentrations of a novel, adipose-specific protein, adiponectin, in type 2 diabetic patients. *Arterioscler Thromb Vasc Biol* 2000;**20**:1595-1599. doi:10.1161/01.ATV.20.6.1595

114. Abassi Z, Goltsman I, Karram T, Winaver J, Hoffman A. Aortocaval fistula in rat: a unique model of volume-overload congestive heart failure and cardiac hypertrophy. *J Biomed Biotechnol* 2011;**2011**:729497. doi:10.1155/2011/729497

115. Fan D, Li L, Wang C, Cui XB, Zhou Y, Wu LL. Adiponectin induces interleukin-6 production and its underlying mechanism in adult rat cardiac fibroblasts. *J Cell Physiol* 2011;**226**:1793-1802. doi:10.1002/jcp.22512

116. Nakamura T, Funayama H, Kudo N, Yasu T, Kawakami M, Saito M, Momomura S, Ishikawa SE. Association of Hyperadiponectinemia With Severity of Ventricular Dysfunction in Congestive Heart Failure. *Circ J* 2006;**70**:1557-1562. doi:10.1253/circj.70.1557

117. Shibata R, Sato K, Kumada M, Izumiya Y, Sonoda M, Kihara S, Ouchi N, Walsh K. Adiponectin accumulates in myocardial tissue that has been damaged by

ischemia-reperfusion injury via leakage from the vascular compartment. *Cardiovasc Res* 2007;**74**:471-479. doi:10.1016/j.cardiores.2007.02.010

118. Guo Z, Xia Z, Yuen VG, McNeill JH. Cardiac expression of adiponectin and its receptors in streptozotocin-induced diabetic rats. *Metabolism* 2007;**56**:1363-1371. doi:10.1016/j.metabol.2007.05.005

119. Jobe LJ, Melendez GC, Levick SP, Du Y, Brower GL, Janicki JS. TNF-alpha inhibition attenuates adverse myocardial remodeling in a rat model of volume overload. *Am J Physiol Heart Circ Physiol* 2009;**297**:H1462-1468. doi:10.1152/ajpheart.00442.2009

120. Kapadia SR, Yakoob K, Nader S, Thomas JD, Mann DL, Griffin BP. Elevated circulating levels of serum tumor necrosis factor-alpha in patients with hemodynamically significant pressure and volume overload. *J Am Coll Cardiol* 2000;**36**:208-212. doi:10.1016/S0735-1097(00)00721-X

121. Kim KY, Kim JK, Jeon JH, Yoon SR, Choi I, Yang Y. c-Jun N-terminal kinase is involved in the suppression of adiponectin expression by TNF-alpha in 3T3-L1 adipocytes. *Biochem Biophys Res Commun* 2005;**327**:460-467. doi:10.1016/j.bbrc.2004.12.026

122. Lim JY, Kim WH, Park SI. GO6976 prevents TNF-alpha-induced suppression of adiponectin expression in 3T3-L1 adipocytes: putative involvement of protein kinase C. *FEBS Lett* 2008;**582**:3473-3478. doi:10.1016/j.febslet.2008.09.012

123. Wang Y, Zhao J, Zhang Y, Lau WB, Jiao LY, Liu B, Yuan Y, Wang X, Tao L, Gao E, Koch WJ, Ma XL. Differential regulation of TNF receptor 1 and receptor 2 in adiponectin expression following myocardial ischemia. *Int J Cardiol* 2013;**168**:2201-2206. doi:10.1016/j.ijcard.2013.01.222

124. Yamauchi T, Nio Y, Maki T, Kobayashi M, Takazawa T, Iwabu M, Okada-Iwabu M, Kawamoto S, Kubota N, Kubota T, Ito Y, Kamon J, Tsuchida A, Kumagai K, Kozono H, Hada Y, Ogata H, Tokuyama K, Tsunoda M, Ide T, Murakami K, Awazawa M, Takamoto I, Froguel P, Hara K, Tobe K, Nagai R, Ueki K, Kadowaki T. Targeted disruption of AdipoR1 and AdipoR2 causes abrogation of adiponectin binding and metabolic actions. *Nat Med* 2007;**13**:332-339. doi:10.1038/nm1557

125. Caselli C, Lionetti V, Cabiati M, Prescimone T, Aquaro GD, Ottaviano V, Bernini F, Mattii L, Del Ry S, Giannessi D. Regional evidence of modulation of cardiac adiponectin level in dilated cardiomyopathy: pilot study in a porcine animal model. *Cardiovasc Diabetol* 2012;**11**:143. doi:10.1186/1475-2840-11-143.

126. Ma Y, Liu Y, Liu S, Qu Y, Wang R, Xia C, Pei H, Lian K, Yin T, Lu X, Sun L, Yang L, Cao Y, Lau WB, Gao E, Wang H, Tao L. Dynamic alteration of adiponectin/adiponectin receptor expression and its impact on myocardial ischemia/reperfusion in type 1 diabetic mice. *Am J Physiol Endocrinol Metab* 2011;**301**:E447-455. doi:10.1152/ajpendo.00687.2010.

127. Li J, Hu X, Selvakumar P, Russell RRr, Cushman SW, Holman GD, Young LH. Role of the nitric oxide pathway in AMPK-mediated glucose uptake and GLUT4 translocation in heart muscle. *Am J Physiol Endocrinol Metab* 2004;**287**:E834-841. doi:10.1152/ajpendo.00234.2004.

128. Wang X, Oka T, Chow FL, Cooper SB, Odenbach J, Lopaschuk GD, Kassiri Z, Fernandez-Patron C. Tumor necrosis factor-alpha-converting enzyme is a key regulator of agonist-induced cardiac hypertrophy and fibrosis. *Hypertension* 2009;**54**:575-582. doi:10.1161/HYPERTENSIONAHA.108.127670

129. Konishi M, Haraguchi G, Ohigashi H, Ishihara T, Saito K, Nakano Y, Isobe M. Adiponectin protects against doxorubicin-induced cardiomyopathy by anti-apoptotic effects through AMPK up-regulation. *Cardiovasc Res* 2011;**89**:309-319. doi:10.1093/cvr/cvq335

130. Liao Y, Takashima S, Maeda N, Ouchi N, Komamura K, Shimomura I, Hori M, Matsuzawa Y, Funahashi T, Kitakaze M. Exacerbation of heart failure in adiponectin-deficient mice due to impaired regulation of AMPK and glucose metabolism. *Cardiovasc Res* 2005;**67**:705-713. doi:10.1016/j.cardiores.2005.04.018

131. Altarejos JY, Taniguchi M, Clanachan AS, Lopaschuk GD. Myocardial ischemia differentially regulates LKB1 and an alternate 5'-AMP-activated protein kinase kinase. *J Biol Chem* 2005;**280**:183-190. doi:10.1074/jbc.M411810200

132. Cleland JG, Daubert JC, Erdmann E, Freemantle N, Gras D, Kappenberger L, Tavazzi L. The effect of cardiac resynchronization on morbidity and mortality in heart failure. *N Engl J Med* 2005;**352**:1539-1549. doi:10.1056/NEJMoa050496

133. Samesima N, Pastore CA, Douglas RA, Filho MM, Pedrosa AA. Improved relationship between left and right ventricular electrical activation after cardiac resynchronization therapy in heart failure patients can be quantified by body surface potential mapping. Clinics (Sao Paulo), 2013:986-991. doi:10.6061/clinics/2013(07)16

134. Sah R, Ramirez RJ, Oudit GY, Gidrewicz D, Trivieri MG, Zobel C, Backx PH. Regulation of cardiac excitation-contraction coupling by action potential repolarization: role of the transient outward potassium current (I(to)). *J Physiol* 2003;**546**:5-18. doi:10.1113/jphysiol.2002.026468

135. Kassiri Z, Zobel C, Nguyen TT, Molkentin JD, Backx PH. Reduction of I(to) causes hypertrophy in neonatal rat ventricular myocytes. *Circ Res* 2002;**90**:578-585.

136. Nanayakkara G, Viswaprakash N, Zhong J, Kariharan T, Quindry J, Amin R. PPARgamma activation improves the molecular and functional components of I(to) remodeling by angiotensin II. *Curr Pharm Des* 2013;**19**:4839-4847. doi:10.2174/1381612811319270006

137. Oh S, Kim KB, Ahn H, Cho HJ, Choi YS. Remodeling of ion channel expression in patients with chronic atrial fibrillation and mitral valvular heart disease. *Korean J Intern Med* 2010;**25**:377-385. doi:10.3904/kjim.2010.25.4.377

138. Gallego M, Alday A, Alonso H, Casis O. Adrenergic regulation of cardiac ionic channels: role of membrane microdomains in the regulation of kv4 channels. *Biochim Biophys Acta* 2014;**1838**:692-699. doi:10.1016/j.bbamem.2013.06.025

139. Yao JA, Jiang M, Fan JS, Zhou YY, Tseng GN. Heterogeneous changes in K currents in rat ventricles three days after myocardial infarction. *Cardiovasc Res* 1999;**44**:132-145. doi:http://dx.doi.org/10.1016/S0008-6363(99)00154-6

140. Smith CC, Yellon DM. Adipocytokines, cardiovascular pathophysiology and myocardial protection. *Pharmacol Ther* 2011;**129**:206-219. doi:10.1016/j.pharmthera.2010.09.003

141. Komatsu M, Ohfusa H, Sato Y, Yajima H, Yamauchi K, Aizawa T, Hashizume K. Strong inverse correlation between serum adiponectin level and heart rate-corrected QT interval in an apparently healthy population: a suggestion for a direct antiatherogenic effect of adiponectin. *Diabetes Care* 2004;**27**:1237-1238. doi:10.2337/diacare.27.5.1237

142. Zhong J, Hwang TC, Adams HR, Rubin LJ. Reduced L-type calcium current in ventricular myocytes from endotoxemic guinea pigs. *Am J Physiol* 1997;**273**:H2312-2324.

143. Barry DM, Trimmer JS, Merlie JP, Nerbonne JM. Differential expression of voltage-gated K+ channel subunits in adult rat heart. Relation to functional K+ channels? *Circ Res* 1995;**77**:361-369. doi:10.1161/01.RES.77.2.361

144. Qin D, Huang B, Deng L, El-Adawi H, Ganguly K, Sowers JR, El-Sherif N. Downregulation of K(+) channel genes expression in type I diabetic cardiomyopathy. *Biochem Biophys Res Commun* 2001;**283**:549-553. doi:10.1006/bbrc.2001.4825

145. Wang Y, Cheng J, Chen G, Rob F, Naseem RH, Nguyen L, Johnstone JL, Hill JA. Remodeling of outward K+ currents in pressure-overload heart failure. *J Cardiovasc Electrophysiol* 2007;**18**:869-875. doi:10.1111/j.1540-8167.2007.00864.x

146. Rosati B, Pan Z, Lypen S, Wang HS, Cohen I, Dixon JE, McKinnon D. Regulation of KChIP2 potassium channel beta subunit gene expression underlies the gradient of transient outward current in canine and human ventricle. *J Physiol* 2001;**533**:119-125. doi:10.1111/j.1469-7793.2001.0119b.x

147. Grubb S, Calloe K, Thomsen MB. Impact of KChIP2 on Cardiac Electrophysiology and the Progression of Heart Failure. *Front Physiol* 2012;**3**:118. doi:10.3389/fphys.2012.00118

148. Foeger NC, Wang W, Mellor RL, Nerbonne JM. Stabilization of Kv4 Protein by the accessory K+ Channel Interacting Protein 2 (KChIP2) subunit is required for

the generation of native myocardial fast transient outward K+ currents. *J Physiol* 2013. doi:10.1113/jphysiol.2013.255836

149. Kapadia SR, Oral H, Lee J, Nakano M, Taffet GE, Mann DL. Hemodynamic regulation of tumor necrosis factor-alpha gene and protein expression in adult feline myocardium. *Circ Res* 1997;**81**:187-195. doi:10.1161/01.RES.81.2.187

150. Torre-Amione G, Kapadia S, Lee J, Durand JB, Bies RD, Young JB, Mann DL. Tumor necrosis factor-alpha and tumor necrosis factor receptors in the failing human heart. *Circulation* 1996;**93**:704-711. doi:10.1161/01.CIR.93.4.704

151. Kleinbongard P, Schulz R, Heusch G. TNFalpha in myocardial ischemia/reperfusion, remodeling and heart failure. *Heart Fail Rev* 2011;**16**:49-69. doi:10.1007/s10741-010-9180-8

152. Kawada H, Niwano S, Niwano H, Yumoto Y, Wakisaka Y, Yuge M, Kawahara K, Izumi T. Tumor necrosis factor-alpha downregulates the voltage gated outward K+ current in cultured neonatal rat cardiomyocytes: a possible cause of electrical remodeling in diseased hearts. *Circ J* 2006;**70**:605-609.

153. Grandy SA, Fiset C. Ventricular K+ currents are reduced in mice with elevated levels of serum TNFalpha. *J Mol Cell Cardiol* 2009;**47**:238-246. doi:10.1016/j.yjmcc.2009.02.025

154. Petkova-Kirova PS, Gursoy E, Mehdi H, McTiernan CF, London B, Salama G. Electrical remodeling of cardiac myocytes from mice with heart failure due to the

overexpression of tumor necrosis factor-alpha. *Am J Physiol Heart Circ Physiol* 2006;**290**:H2098-2107. doi:10.1152/ajpheart.00097.2005

155. Breidthardt T, Christ M, Matti M, Schrafl D, Laule K, Noveanu M, Boldanova T, Klima T, Hochholzer W, Perruchoud AP, Mueller C. QRS and QTc interval prolongation in the prediction of long-term mortality of patients with acute destabilised heart failure. *Heart* 2007;**93**:1093-1097. doi:10.1136/hrt.2006.102319

156. Vrtovec B, Delgado R, Zewail A, Thomas CD, Richartz BM, Radovancevic B. Prolonged QTc interval and high B-type natriuretic peptide levels together predict mortality in patients with advanced heart failure. *Circulation* 2003;**107**:1764-1769. doi:10.1161/01.CIR.0000057980.84624.95

157. Maeder MT, Ammann P. Changes in BNP and QTc for prediction of sudden death in heart failure. *Future Cardiol* 2013;**9**:317-320. doi:10.2217/fca.13.11

158. Arking DE, Pulit SL, Crotti L, van der Harst P, Munroe PB, Koopmann TT, Sotoodehnia N, Rossin EJ, Morley M, Wang X, Johnson AD, Lundby A, Gudbjartsson DF, Noseworthy PA, Eijgelsheim M, Bradford Y, Tarasov KV, Dorr M, Muller-Nurasyid M, Lahtinen AM, Nolte IM, Smith AV, Bis JC, Isaacs A, Newhouse SJ, Evans DS, Post WS, Waggott D, Lyytikainen LP, Hicks AA, Eisele L, Ellinghaus D, Hayward C, Navarro P, Ulivi S, Tanaka T, Tester DJ, Chatel S, Gustafsson S, Kumari M, Morris RW, Naluai AT, Padmanabhan S, Kluttig A, Strohmer B, Panayiotou AG, Torres M, Knoflach M, Hubacek JA, Slowikowski K, Raychaudhuri S, Kumar RD, Harris TB, Launer LJ, Shuldiner AR, Alonso A,

Bader JS, Ehret G, Huang H, Kao WH, Strait JB, Macfarlane PW, Brown M, Caulfield MJ, Samani NJ, Kronenberg F, Willeit J, Consortium CA, Consortium C, Smith JG, Greiser KH, Meyer Zu Schwabedissen H, Werdan K, Carella M, Zelante L, Heckbert SR, Psaty BM, Rotter JI, Kolcic I, Polasek O, Wright AF, Griffin M, Daly MJ, Dcct/Edic, Arnar DO, Holm H, Thorsteinsdottir U, e MC, Denny JC, Roden DM, Zuvich RL, Emilsson V, Plump AS, Larson MG, O'Donnell CJ, Yin X, Bobbo M, D'Adamo AP, Iorio A, Sinagra G, Carracedo A, Cummings SR, Nalls MA, Jula A, Kontula KK, Marjamaa A, Oikarinen L, Perola M, Porthan K, Erbel R, Hoffmann P, Jockel KH, Kalsch H, Nothen MM, Consortium H, den Hoed M, Loos RJ, Thelle DS, Gieger C, Meitinger T, Perz S, Peters A, Prucha H, Sinner MF, Waldenberger M, de Boer RA, Franke L, van der Vleuten PA, Beckmann BM, Martens E, Bardai A, Hofman N, Wilde AA, Behr ER, Dalageorgou C, Giudicessi JR, Medeiros-Domingo A, Barc J, Kyndt F, Probst V, Ghidoni A, Insolia R, Hamilton RM, Scherer SW, Brandimarto J, Margulies K, Moravec CE, del Greco MF, Fuchsberger C, O'Connell JR, Lee WK, Watt GC, Campbell H, Wild SH, El Mokhtari NE, Frey N, Asselbergs FW, Mateo Leach I, Navis G, van den Berg MP, van Veldhuisen DJ, Kellis M, Krijthe BP, Franco OH, Hofman A, Kors JA, Uitterlinden AG, Witteman JC, Kedenko L, Lamina C, Oostra BA, Abecasis GR, Lakatta EG, Mulas A, Orru M, Schlessinger D, Uda M, Markus MR, Volker U, Snieder H, Spector TD, Arnlov J, Lind L, Sundstrom J, Syvanen AC, Kivimaki M, Kahonen M, Mononen N, Raitakari OT, Viikari JS,

Adamkova V, Kiechl S, Brion M, Nicolaides AN, Paulweber B, Haerting J, Dominiczak AF, Nyberg F, Whincup PH, Hingorani AD, Schott JJ, Bezzina CR, Ingelsson E, Ferrucci L, Gasparini P, Wilson JF, Rudan I, Franke A, Muhleisen TW, Pramstaller PP, Lehtimaki TJ, Paterson AD, Parsa A, Liu Y, van Duijn CM, Siscovick DS, Gudnason V, Jamshidi Y, Salomaa V, Felix SB, Sanna S, Ritchie MD, Stricker BH, Stefansson K, Boyer LA, Cappola TP, Olsen JV, Lage K, Schwartz PJ, Kaab S, Chakravarti A, Ackerman MJ, Pfeufer A, de Bakker PI, Newton-Cheh C. Genetic association study of QT interval highlights role for calcium signaling pathways in myocardial repolarization. *Nat Genet* 2014;**46**:826-836. doi:10.1038/ng.3014

159. Greenstein JL, Wu R, Po S, Tomaselli GF, Winslow RL. Role of the calcium-independent transient outward current I(to1) in shaping action potential morphology and duration. *Circ Res* 2000;**87**:1026-1033. doi:10.1161/01.RES.87.11.1026

160. Oudit GY, Kassiri Z, Sah R, Ramirez RJ, Zobel C, Backx PH. The molecular physiology of the cardiac transient outward potassium current (I(to)) in normal and diseased myocardium. *J Mol Cell Cardiol* 2001;**33**:851-872. doi:10.1006/jmcc.2001.1376

161. Kaprielian R, Wickenden AD, Kassiri Z, Parker TG, Liu PP, Backx PH. Relationship between K+ channel down-regulation and [Ca2+]i in rat ventricular

myocytes following myocardial infarction. *J Physiol* 1999;**517 (Pt 1)**:229-245. doi:10.1111/j.1469-7793.1999.0229z.x

162. Jin H, Hadri L, Palomeque J, Morel C, Karakikes I, Kaprielian R, Hajjar R, Lebeche D. KChIP2 attenuates cardiac hypertrophy through regulation of Ito and intracellular calcium signaling. *J Mol Cell Cardiol* 2010;**48**:1169-1179. doi:10.1016/j.yjmcc.2009.12.019

163. Ouchi N, Kihara S, Arita Y, Okamoto Y, Maeda K, Kuriyama H, Hotta K, Nishida M, Takahashi M, Muraguchi M, Ohmoto Y, Nakamura T, Yamashita S, Funahashi T, Matsuzawa Y. Adiponectin, an adipocyte-derived plasma protein, inhibits endothelial NF-kappaB signaling through a cAMP-dependent pathway. *Circulation* 2000;**102**:1296-1301. doi:10.1161/01.CIR.102.11.1296

164. Gonon AT, Widegren U, Bulhak A, Salehzadeh F, Persson J, Sjoquist PO, Pernow J. Adiponectin protects against myocardial ischaemia-reperfusion injury via AMP-activated protein kinase, Akt, and nitric oxide. *Cardiovasc Res* 2008;**78**:116-122. doi:10.1093/cvr/cvn017

165. Fernandez-Velasco M, Ruiz-Hurtado G, Hurtado O, Moro MA, Delgado C. TNF-alpha downregulates transient outward potassium current in rat ventricular myocytes through iNOS overexpression and oxidant species generation. *Am J Physiol Heart Circ Physiol* 2007;**293**:H238-245. doi:10.1152/ajpheart.01122.2006